



HAL
open science

Fluvial terrace formation in mountainous areas: (1) Influence of climate changes during the last glacial cycle in Albania

Oswaldo Guzmán, Jean-Louis Mugnier, Riccardo Vassallo, Rexhep Koçi, Julien Carcaillet, François Jouanne

► **To cite this version:**

Oswaldo Guzmán, Jean-Louis Mugnier, Riccardo Vassallo, Rexhep Koçi, Julien Carcaillet, et al.. Fluvial terrace formation in mountainous areas: (1) Influence of climate changes during the last glacial cycle in Albania. *Comptes Rendus. Géoscience*, 2024, 355 (G2), pp.331-353. <10.5802/crgeos.251>. <hal-04639660>

HAL Id: hal-04639660

<https://hal.science/hal-04639660v1>

Submitted on 9 Jul 2024

HAL is a multi-disciplinary open access archive for the deposit and dissemination of scientific research documents, whether they are published or not. The documents may come from teaching and research institutions in France or abroad, or from public or private research centers.

L'archive ouverte pluridisciplinaire **HAL**, est destinée au dépôt et à la diffusion de documents scientifiques de niveau recherche, publiés ou non, émanant des établissements d'enseignement et de recherche français ou étrangers, des laboratoires publics ou privés.



HAL Authorization

1 **Fluvial terrace formation in mountainous areas:**
2 **(1) Influence of climate changes during the last glacial cycle in Albania**
3
4

5 Oswaldo Guzmán^{a,b}, Jean-Louis Mugnier^{b*}, Riccardo Vassallo^b, Rexhep Koçi^c, Julien Carcaillet^b, François
6 Jouanne^b

7 ^a Grupo de Investigación en Ciencias de La Tierra y Clima, Universidad Regional Amazónica Ikiam, Muyuna,
8 Ecuador.

9 ^b ISTERre, Université Grenoble Alpes, Université Savoie Mont Blanc, CNRS, IRD, Le Bourget du Lac, France.

10 ^c Institute of Geosciences of the Polytechnical University of Tirana, Albania

11 * Corresponding author: Jean-Louis Mugnier - E-mail address: jemug@univ-smb.fr
12

13 **Abstract:** This work analyses terraces formation from the case of Albanian rivers. An
14 allostratigraphy study of the fluvial terraces is combined with new numerical dating. $30\ ^{14}\text{C}$ and
15 $4\ ^{10}\text{Be}$ new dated sites along four rivers and 45 ages previously acquired along three other rivers
16 were used to define terrace chronologies at the scale of the whole Albania. Few terrace remnants
17 are related to stages older than the last glacial period and are older than 194 ± 19 ka. Terrace
18 level (T1) includes plain-like terraces and T1 is related to a rapid succession of valley incision
19 and valley fill that occurred during the warm Holocene climatic optimum. The other nine terrace
20 levels (T2 to T10) formed during the last glacial period (MIS 5d to end of MIS 2). Terraces T2,
21 T6 and T7 formed nearly synchronously with interstadial transitions toward warmer and wetter
22 conditions. The formation of terraces T3, T4, T5 and T8 (<60ka) coincide with the warm
23 climatic excursions of the Heinrich events. This result suggests that these short climatic events
24 strongly punctuate the geomorphologic dynamics of rivers in mountainous areas.
25

26 **Keywords:** Albania, fluvial sedimentation, terraces, climatic and vegetation controls, river
27 piracy, late glacial cycle, interstadials, *in situ* produced ^{10}Be dating, ^{14}C dating, continental
28 sediment
29

30

31 **I Introduction**

32 A huge body of published works (e.g. see the bibliography in Cordier et al., 2017)
33 suggests that the formation of river terraces, defined as flat surfaces above fluvial sediment, is
34 affected by climate. It has been demonstrated that, in general, river incision took place at climatic
35 transitions (e.g. Vandenberghe, 2003, 2015; Bridgland and Westaway, 2008; Antoine et al.,
36 2016). Nonetheless, numerous studies show that terraces are not a simple climatic proxy (Cordier
37 et al., 2017; Schanz et al., 2018; Pazzaglia, 2022) and numerous processes interact together in
38 terrace formation (Starkel, 1994; Vandenberghe, 2003, 2015). Furthermore, it has been stressed
39 that climatic variations must cross thresholds of duration or magnitude to induce changes
40 between erosion and deposition (e.g. Schumm, 1979; Vandenberghe, 2003). The role of the
41 succession of the glacial/interglacial periods is classically described for major fluctuations at 10^5
42 years scale (e.g. Starkel, 1994; Riser, 1999). However, the role of shorter time scale climatic
43 fluctuations is frequently discussed from the compilation of geochronologic studies distributed
44 on very large areas (Pazzaglia, 2022) but is usually poorly evidenced along single rivers
45 (Woodward et al., 2008).

46 Terrace levels, formed during the last glacial cycle, are widely preserved along all the
47 Albanian rivers (Woodward et al., 2008; Carcaillet et al., 2009; Koçi et al., 2018). Albanian river
48 catchments (**Figure 1**) are located in an area where large-scale controls (climate, tectonics or
49 eustatism) can be considered similar: the climate is Mediterranean (Ozenda, 1975), the tectonics
50 is controlled by the Adriatic subduction beneath southeastern Europe (Roure et al., 2004) and all
51 rivers have the same base level fluctuations linked to the eustatism (Lambeck and Chappell,
52 2001).

53 Many studies have already described the general morphology of terraces (Melo, 1961;
54 Prifti, 1981; Prifti, 1984; Prifti and Meçaj, 1987; Lewin et al., 1991; Woodward et al., 2008) and
55 other studies have focused on the history of incision/uplift (Carcaillet et al., 2009; Guzman et
56 al., 2013; Gemignani et al., 2022). But to make progress in understanding the genesis of terraces,
57 numerical chronological constraints are necessary and are therefore proposed in this article.

58 There was few ages for the river terraces preserved in the central and northern part of
59 Albania. Four ^{10}Be and 21 ^{14}C new terrace ages, as well as geomorphological data, are reported
60 in this paper. These data are combined with previous results in order to furnish an
61 allostratigraphic/chronologic framework for the unit deposition and terrace formation during
62 the past 200 ka along 7 Albanian rivers. This enriched database supported by 70 numerical ages
63 is used to discuss the influence of climate changes on the genesis of terraces.



Fig. 1

65
 66 **Figure 1.** The rivers of Albania. a) Topographic map of Albania derived from the 90-m Shuttle Radar
 67 Topography Mission (SRTM) digital elevation model. Watersheds of the seven main Albanian rivers are
 68 bounded by black dashed lines. Dark diamonds indicate published data (Lewin et al., 1991; Hamlin et
 69 al., 2000; Woodward et al., 2001, 2008; Carcaillet et al., 2009; Guzmán et al., 2013; Koçi et al., 2018),
 70 yellow circles (^{14}C dating) and green stars (^{10}Be dating) indicate the data obtained in this study. The
 71 boxes show the location of Supplementary Information, **Appendix 5** and **Figure 7**. Core 1202 and 1204
 72 in the Ohrid and Prespa lakes refer to the work of Wagner et al. (2009, 2010; see **Figure 9**).

73

74 2. Methodology

75 Field surveys have been performed along all the rivers and the allostratigraphic units
76 (Hughes, 2010) were defined from an analysis of the lithostratigraphy and the geometry of the
77 interface between Quaternary sediment and bedrock. Thicknesses and characteristics of the
78 sedimentary units were observed in approximately one thousand sites. The terrace extension at
79 large scale was mapped on the basis of field observations reported on topographic maps at the
80 1:25000 scale (Institutin Topografik te Ushtrise Tirane, 1959–1990), 30-m digital elevation
81 models (SRTM, 2013) and satellite images (image@2023CNES/Airbus, available on Google
82 Earth).

83

84 **2.2 Dating of sedimentary units and terrace surfaces**

85 In a first step, the relative chronology of the terraces was deduced for each river from
86 the geometric relationship between the mapped terraces (Prifti, 1981; Prifti, 1984; Prifti and
87 Meçaj, 1987). The correlation between the terrace remnants was performed by reconstructing a
88 regular paleo-river profile from the upstream to downstream zones (Guzman et al., 2013).

89 Although some relative methods, such as those based on the soil chronosequence, can
90 differentiate the age of Middle Pleistocene sequences (Rowey and Siemens, 2021), they were
91 not used in this work: in the studied area, a dozen levels of terraces are distributed over a time
92 period spanning one hundred thousand years (Carcaillet et al, 2009), a temporal distribution not
93 favorable to the use of surface alteration as a time indicator (Rixhon, 2022). Furthermore, it has
94 been shown that numeric dating is the best way to compare terrace chronologies at a large scale
95 (Woodward et al., 2008) and that absolute dating techniques are necessary to correlate terraces
96 with climatic stages (Schaller et al., 2016).

97 In a second step, the numeric ages of the terraces were determined. New data were based
98 on radiocarbon (^{14}C) and *in situ* produced ^{10}Be dating. (see **Supplementary Information,**
99 **Appendix 1 and Appendix 2** for technical details).

100 The ^{14}C ages represent the death of organic material. Samples consist of plant remains
101 or charcoal, a few millimeters in size (**Supplementary Information, Figure 1b in Appendix**
102 **1**), which are transported rapidly by rivers. Although there may be a delay between plant death
103 and final deposition, we consider ^{14}C ages to represent the age of sediment deposition. In order
104 to exclude an eolian origin, that has sometimes been suggested in the Mediterranean area for
105 the formation of the upper sub-unit of fine-grained deposits (Woodward et al., 2008; Obreht et
106 al., 2014; Cremaschi et al., 2015), the samples were taken from deposits also containing some
107 coarse sands and small gravels or from fine-grained lenses within the coarse material
108 (**Supplementary Information, Figure 1c, Appendix 1**). Therefore most ^{14}C samples were

109 collected close to the bottom of the upper sub-unit (see **Supplementary information, Figure**
 110 **1a, Appendix1**).

111
 112 **Table 1. Results of the ^{10}Be analysis (see Figure 6 and the Supplementary Information,**
 113 **Appendix 2)). The depth profiles are from $T3_{(pa)}$ and $T8_{(ma)}$ (location of Shk-10 and Ma-03 on the**
 114 **Supplementary Information, Appendix 5 and Figure 7, respectively). Samples Ma-04 and Ma-06 are**
 115 **amalgamated clasts collected at the top surface of terraces $T8_{(ma)}$ and $T9_{(ma)}$, respectively (location on**
 116 **Figure 7).**

117

Sample	Type of sample	Lithology	Latitude (°N)	Longitude (°E)	Altitude (m)	Depth (cm)	Shielding factor	^{10}Be concentration (10^5 at/g)	^{10}Be age (ka)	Terrace
Lower paleo-Devoll										
Shk-10	Cobble	Quartzite	41.0618	19.8685	65	30	0.998	0.77 ± 0.07	18.81 ± 2.4	$T3_{(pa)}$
Shk-11	Cobble	Granite				47		0.21 ± 0.05		
Shk-12	Amalgam pebbles	Heterogeneous				75		0.61 ± 0.03		
Shk-14	Cobble	Granite				157		0.47 ± 0.06		
Shk-16	Cobble	Granite				240		0.66 ± 0.05		
Mat river - Uzal Dam										
Ma-03	Amalgam pebbles	Heterogeneous	41.6748	19.9166	183	10	0.998	4.40 ± 0.14	100.8 ± 9.4	$T8_{(ma)}$
Ma-09	Amalgam pebbles	Heterogeneous				285		0.52 ± 0.06		
Ma-08	Amalgam pebbles	Heterogeneous				495		0.27 ± 0.02		
Ma-07	Amalgam pebbles	Heterogeneous				590		0.26 ± 0.01		
Mat river - Livadhi										
Ma-04	Amalgam pebbles	Heterogeneous	41.5920	20.0336	262	0	1	5.63 ± 0.16	$\geq 112.32 \pm 10.3$	$T8_{(ma)}$
Mat river - Burrel										
Ma-06	Amalgam pebbles	Heterogeneous	41.6042	20.0130	322	0	1	10.04 ± 0.40	$\geq 193.92 \pm 19.3$	$T9_{(ma)}$

118
 119
 120 The ^{10}Be ages represent the exposure ages of the terrace surfaces (Gosse and Phillips,
 121 2001). The ^{10}Be concentration on the terrace surface was measured in samples formed of
 122 amalgamated quartz clasts less than 5 cm in length. The attenuation of ^{10}Be at depth was
 123 analysed by sampling cobble samples along one profile and amalgamated pebbles samples
 124 along another one (Gosse and Phillips, 2001); the best fit profiles and their uncertainties were
 125 then calculated using a Monte Carlo approach (Hidy et al., 2010) (**Table 1**). In addition to the
 126 new ^{10}Be ages, the previously published ^{10}Be ages were re-calibrated following the same
 127 procedure (**Table 2**).

128
 129 **Table 2. Numeric ages from fluvial terraces of Albania.**

130 ^a Samples: (*) for a cosmogenic depth profile, only the age of the surface and the depth of the shallowest
 131 sample are given.

132 ^b Type of material dated: C = charcoal, Vd = vegetal debris, Cc = calcite cement, S = sediment, Dt =
 133 deer tooth, Sr = siliceous rock, Ca = Calcereous rock.

134 ^c Location from GPS coordinates or (ç) estimated from published maps.

135 ^d Dating method: ^{14}C = radiocarbon, TL = thermoluminescence, U/Th = uranium series, ESR = electron
 136 spin resonance, ^{10}Be and ^{36}Cl = cosmogenic in situ produced data.

137 ^e Numerical ages: all ^{10}Be ages have been calculated (**Table 1**) or recalculated with the parameters
 138 indicated in Appendix 2. All ^{14}C ages have been estimated from the IntCal 13 calibrated intervals and
 139 the oldest (§) were also corrected using the polynomial calibration of Bard et al. (2004). (£) Have not
 140 been considered for the probability density curves due to their large uncertainty.

141 ^f Source: (1) Guzmán et al. (2013), (2) Carcaillet et al. (2009), (3) Lewin et al. (1991), (4) Woodward et
 142 al. (2008), (5) Hamlin et al. (2000), (6) Koçi et al. (2018), (7) Gemignani et al. (2022).

Sample ^a		Latitude (°N) ^c	Long. (°E) ^c	Sample elevation above the river (m)	Sample depth below the surface (m)	Method ^d	Lab-Code Reactor Reference	¹⁴ C Ages (ka)	Calibrated interval ¹⁴ C Cal ka BP (Probability=0.95)	Ages (ka) ^e	Local terrace name	Regional terrace name	Source ^f
Vjosa													
A153	C	40.2076	20.3875	17.3	0.7	¹⁴ C	SacA 16001	190 ± 30	32 - 302	-	-	colluv.	This study
A150	C	40.2084	20.0934	9.5	0.5	¹⁴ C	SacA 15998	330 ± 30	308 - 473	-	-	colluv.	(1)
A28	Vd	40.3354	19.9921	12	2	¹⁴ C	Poz-8824	705 ± 30	565 - 691	-	-	colluv.	(1)
OxA-192	C	39.97(ç)	20.66(ç)	~4.5	<1	¹⁴ C	OxA-192	800 ± 100	560 - 928	-	T1(vj)	T0	(3)
OxA-191	C	40.87(ç)	21.65(ç)	~4.5	<1	¹⁴ C	OxA-191	1000 ± 50	789 - 1049	-	T1(vj)	T0	(3)
A155	Vd	40.3611	19.9907	13.4	4	¹⁴ C	SacA 16002	3870 ± 60	4094 - 4436	-	-	colluv.	(1)
OxA-5246	C	39.96(ç)	20.65(ç)	~10.6	~0.1	¹⁴ C	OxA-5246	13810 ± 130	16291 - 17116	-	T3(vj)	T3	(4)
Beta-109162	C	39.96(ç)	20.65(ç)	~10.6	~0.1	¹⁴ C	Beta-109162	13960 ± 260	16203 - 17647	-	T3(vj)	T3	(4)
Beta-109187	C	39.96(ç)	20.65(ç)	~10.4	~0.4	¹⁴ C	Beta-109187	14310 ± 200	16865 - 17947	-	T3(vj)	T3	(4)
VOI24	S	39.94(ç)	20.71(ç)	~9.7	<1	TL	VOI24	-	-	19.60 ± 3.00	T3(vj)	T3	(3)
Tributary site	Cc	39.95(ç)	20.68(ç)	~10.5	~1.6	U/Th	-	-	-	21.25 ± 2.50	T3(vj)	T3	(5)
Old Klithonia	Cc	39.96(ç)	20.65(ç)	~9.3	~2.3	U/Th	-	-	-	24.00 ± 2.00	T4(vj)	T4	(5)
571c	Dt	39.96(ç)	20.68(ç)	~12.4	~7.5	ESR	571c	-	-	24.30 ± 2.60	T4(vj)	T4	(3)
571a	Dt	39.96(ç)	20.68(ç)	~12.4	~7.5	ESR	571a	-	-	25.00 ± 0.50	T4(vj)	T4	(3)
Old Klithonia	Cc	39.96(ç)	20.65(ç)	~9.3	~5	U/Th	-	-	-	25.00 ± 2.00	T4(vj)	T4	(5)
571b	Dt	39.96(ç)	20.68(ç)	~12.4	~7.5	ESR	571b	-	-	26.00 ± 1.90	T4(vj)	T4	(3)
VOI23	S	39.96(ç)	20.68(ç)	~12.4	<1	TL	VOI23	-	-	28.00 ± 7.10 (£)	T4(vj)	T4	(3)
A151	C	40.2140	20.3842	21.7	0.3	¹⁴ C	SacA 15999	24070 ± 150	27783 - 28848	-	T5(vj)	T5	This study
Konitsa1	Cc	39.86(ç)	20.77(ç)	~10	~1-1.5	U/Th	-	-	-	53.00 ± 4.00	T6(vj)	T8	(5)
Konitsa2	Cc	39.86(ç)	20.77(ç)	~10	~1-1.5	U/Th	-	-	-	56.50 ± 5.00	T6(vj)	T8	(5)
Konitsa3	Cc	39.86(ç)	20.77(ç)	~11	~1-1.5	U/Th	-	-	-	74.00 ± 6.00	T7(vj)	T9	(5)
Konitsa4	Cc	39.86(ç)	20.77(ç)	~12.7	~1-1.5	U/Th	-	-	-	80.00 ± 7.00	T7(vj)	T9	(5)
Konitsa5	Cc	39.86(ç)	20.77(ç)	~15.5	~1-1.5	U/Th	-	-	-	113.00 ± 6.00	T8(vj)	T10	(5)
VOI26	S	39.86(ç)	20.77(ç)	~56	~22	TL	VOI26	-	-	>150 (£)	T9(vj)	T12	(3)
Osum													
A17	Vd	40.4508	20.2808	17	2	¹⁴ C	Poz-10576	9990 ± 50	11263 - 11705	-	T2(os)	T2	(2)
Par-0 (*)	Sr	40.5200	20.7200	70	0	¹⁰ Be	-	-	-	19.25 ± 1.3	T3(os)	T3	(2)
Quaf-0 (*)	Sr	40.5500	20.6900	29	0	¹⁰ Be	-	-	-	20.33 ± 1.5	T3(os)	T3	(2)
A16	Vd	40.6394	20.0553	24	4	¹⁴ C	Poz-10575	29900 ± 1300	31323 - 37457	-	T5(os)	T6	(2)
A83	C	40.6800	20.0200	14.8	3.7	¹⁴ C	Poz-13850	37000 ± 300	41036 - 42066	-	T6(os)	T7	(2)
A18	Vd	40.5600	20.1400	53	6	¹⁴ C	Poz-10578	45300 ± 1600	> 46237	50.70 ± 1.80 (\$)	T7(os)	T8	(2)
A14	Vd	40.6403	20.0575	33.8	1.2	¹⁴ C	Poz-10574	49000 ± 2500	> 49928	54.40 ± 2.78 (\$)	T7(os)	T8	(2)
Grem-0(*)	Sr	40.5560	20.7383	50	0	¹⁰ Be	-	-	-	54.01 ± 3.0	T7(os)	T8	(2)
Paleo-Devoll													
A05	Vd	40.9092	20.1393	34	2	¹⁴ C	Poz-10572	119.5 ± 0.3 pMC	-	modern	-	colluv.	This study
Cer-08	C	41.0275	19.9817	8.4	0.6	¹⁴ C	Poz-39495	30 ± 80	9 - 275	-	-	colluv.	(1)
Dev-02	C	40.9910	20.0165	16.6	0.5	¹⁴ C	Poz-39496	540 ± 130	306 - 727	-	-	colluv.	(1)
Shk-06	Vd	41.0663	19.8800	52.8	2.2	¹⁴ C	Poz-34987	162 ± 0.46 pMC	-	modern	-	colluv.	This study
Shk-22	C	41.0649	19.8714	6.3	0.7	¹⁴ C	Poz-39201	90 ± 30	22 - 266	-	-	colluv.	This study
Cer-01	C	41.0100	20.0083	8.4	1.6	¹⁴ C	Poz-39197	5400 ± 40	6021 - 6293	-	T2(pa)	T1	This study
Shk-10(*)	Sr	41.0618	19.8685	14.7	0.3	¹⁰ Be	-	-	-	18.81 ± 2.4	T3(pa)	T3	This study
A60	C	40.9676	20.0526	19	0.5	¹⁴ C	Poz-12223	17640 ± 160	20895 - 21800	-	T3(pa)	T3	(1)
A58	C	40.9214	20.1292	15.7	3	¹⁴ C	Poz-12116	21850 ± 150	25815 - 26437	-	T4(pa)	T4	(1)
A100	C	40.9660	20.0636	24	1	¹⁴ C	Poz-17242	22780 ± 200	26583 - 27490	-	T4(pa)	T4	(1)
A8	Vd	40.8271	20.2154	42.5	5	¹⁴ C	Poz-9838	23760 ± 150	27580 - 28163	-	T5(pa)	T5	(1)
A1	Vd	40.8836	20.1773	42	6	¹⁴ C	Poz-8816	25500 ± 300	28921 - 30498	-	T5(pa)	T5	This study
A61	C	40.9414	20.1089	41.2	1	¹⁴ C	Poz-12117	38900 ± 700	41939 - 44142	-	T7(pa)	T7	This study
A56A	C	40.8834	20.1764	41	3	¹⁴ C	-	> 52000	-	> 52	T8(pa)	T8	This study
Erzen													
A41	C	41.2697	19.8400	3	1.5	¹⁴ C	Poz-8826	170 ± 30	35 - 291	-	-	colluv.	(6)
A11	C	41.2900	19.7100	3.4	0.8	¹⁴ C	Poz-8818	200 ± 30	25 - 304	-	-	colluv.	(6)
A81	C	41.2866	19.7094	23.4	1	¹⁴ C	Poz-13849	275 ± 35	152 - 459	-	-	colluv.	This study
A65	C	41.3088	19.7544	29	0.8	¹⁴ C	Poz-12784	500 ± 30	501 - 617	-	-	colluv.	This study
A76	Vd	41.2800	19.8300	11.7	1	¹⁴ C	Poz-13847	3075 ± 35	3182 - 3372	-	-	colluv.	This study
A63B	C	41.2870	19.7197	17	3	¹⁴ C	Poz-12118	3700 ± 35	3927 - 4150	-	-	colluv.	This study
A13	C	41.2700	19.6400	9	0.4	¹⁴ C	Poz-8823	1660 ± 30	1421 - 1690	-	T1(er)	T0	(6)
A12	C	41.2700	19.6400	9	1	¹⁴ C	Poz-10573	1730 ± 30	1564 - 1708	-	T1(er)	T0	This study
A42	Vd	41.2700	19.8000	12	1	¹⁴ C	Poz-8827	6840 ± 60	7578 - 7817	-	T2(er)	T1	(6)
A115	C	41.2844	19.9683	17	0.8	¹⁴ C	Poz-17243	26600 ± 500	29631 - 31465	-	T3(er)	T5	This study
A67	C	41.2700	19.6400	9.4	3	¹⁴ C	Poz-12120	30400 ± 300	33889 - 34912	-	T4(er)	T6	This study
A69	C	41.2900	19.6400	41	1.2	¹⁴ C	Poz-12121	31500 ± 400	34671 - 36231	-	T4(er)	T6	(6)
A64	C	41.2700	19.7100	24.8	0.8	¹⁴ C	Poz-12224	33400 ± 500	36358 - 38827	-	T4(er)	T6	This study
A79	C	41.2900	19.7100	26.5	2	¹⁴ C	Poz-13848	44200 ± 1600	>45447	49.59 ± 1.76(\$)	T6(er)	T8	This study
A70	C	41.2900	19.6000	22	0.5	¹⁴ C	Poz-12785	48000 ± 2000	>49910	53.40 ± 2.22(\$)	T6(er)	T8	(6)
Mat													
Ma-05	C	41.6178	20.0294	24.3	0.7	¹⁴ C	Poz-34984	1075 ± 30	931 - 1056	-	-	colluv.	This study
Ma-18	C	41.6245	19.9978	7	0.7	¹⁴ C	Poz-39198	1725 ± 30	1562 - 1706	-	T1(m)	T0	This study
Ma-21	C	41.6246	19.9970	10.3	0.7	¹⁴ C	Poz-39199	5100 ± 40	5746 - 5922	-	T2(m)	T1	This study
Ma-24	C	41.6273	19.9968	26	2.1	¹⁴ C	Poz-39200	14850 ± 80	17856 - 18296	-	T3(m)	T3	This study
Ma-04(*)	Sr	41.5920	20.0336	100	0	¹⁰ Be	-	-	-	100.8 ± 9.4	T8(m)	T10	This study
Ma-03	Sr	41.6748	19.9166	94	0.1	¹⁰ Be	-	-	-	≥112.32 ± 10.3	T8(m)	T10	This study
Ma-06	Sr	41.6042	20.0130	190	0	¹⁰ Be	-	-	-	≥193.92 ± 19.3	T9(m)	T11	This study
Drin													
TPN(*)	Ca	42.37855	20.08971	12	0.5	³⁶ Cl	-	-	-	8.2 (-2/+4)	T2(dr)	T1	(7)
TPS(*)	Ca	42.34380	20.11545	56	0.4	³⁶ Cl	-	-	-	12.3 (-2/+5)	T3(dr)	T2	(7)

144 The limestone pebble-rich terraces of the Drin River (Gemignani et al., 2022) have been
145 dated using ^{36}Cl . Other ages (Lewin et al., 1991; Woodward et al., 2008) refer to the mineral
146 formation (U/Th) or the time without daylight exposure (ESR and TL) within the alluvium and
147 are older than the ultimate phases of river aggradation (Noller et al., 2000).

148

149 **3. Setting**

150

151 **3.1. Climate and paleoclimate of Albania**

152 Albania's present climate is Mediterranean on the coast, with 2 to 3 hot, dry months in
153 summer and 4 to 5 mild, rainy months in winter. In the mountainous regions, the climate is
154 continental with cold and snow-covered winters.

155 The paleo climatic records for the last 500 ka were studied in the region in Lake Ohrid,
156 (Sadori et al., 2016) and Lake Ioannina (Roucoux et al., 2008) (location on **Figure 1**). These
157 local records correspond well with the results found in the isotope record of Greenland (Grootes
158 et al., 1993) or in the marine records of the Iberian margin (de Abreu et al., 2003) and the eastern
159 Mediterranean (Konijnendijk et al., 2015). They show a succession of cold periods followed by
160 rapid warm excursions (Clement and Paterson, 2008).

161 The Adriatic Sea, which controls the base level of Albania's rivers, was affected by
162 eustatic fluctuations which are tuned to the global sea level variations and ranged from -120 m
163 to +10 m during the last glacial period (Lambeck and Chappell, 2001). Colder sea surface
164 temperatures that occurred in the Mediterranean Sea (Cacho et al., 1999; Sánchez Goñi et al.,
165 2002; Geraga et al., 2005) during Marine Isotope Stages (MIS) 5 to 2 were linked to the polar
166 water that entered through the Strait of Gibraltar and were closely related to ice rafting events
167 in the northeast Atlantic, called Heinrich events (HEs) (Heinrich, 1988). These short cold events
168 (one to two thousand years; Chappell, 2002; Ziemer et al., 2019) or even less (Bond et al.,
169 1992; Hemming, 2004) were always followed by warm periods (Rahmstorf, 2002). Therefore,
170 the temperature evolution of the Albanian region at the millennial scale is similar to that of the
171 north Atlantic domain (e.g. Sánchez Goñi et al., 2002, Tzedakis et al., 2004).

172 The climatic-water-balance of the landscape (ratio between rainfall, runoff,
173 evapotranspiration, etc.) induces complex connection between temperature and precipitation
174 within the region and a decline in precipitation probably occurred in the western Mediterranean
175 Sea during the Heinrich events. They induced cooler sea surface temperatures that inhibited the
176 moisture supply to the atmosphere (Kallel et al., 1997, 2000) whereas increased rainfalls in the

177 western Mediterranean region are evidenced during warm intervals by the sapropel records
178 (Toucanne et al., 2015).

179 Thus, it is expected that high-frequency Heinrich events induced rapid climatic changes
180 in the Mediterranean region with a succession of dry and cold events followed by rapid warming
181 and moisture return (Toucanne et al., 2015). Lacustrine sediments in eastern Albania also
182 recorded HEs-induced climatic changes through proxies of the alteration, like a high
183 concentration of manganese and total inorganic carbon (Wagner et al., 2010) and a high
184 zirconium/titanium ratio (Wagner et al., 2009).

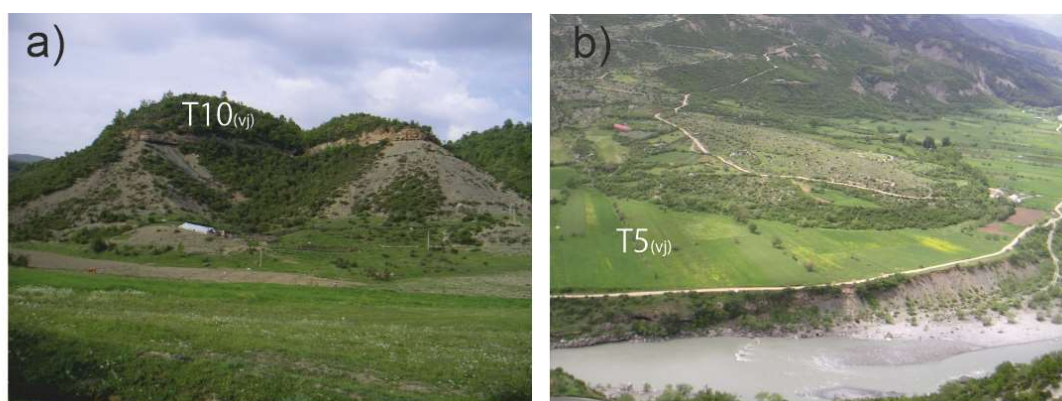
185

186 **3.2. Geology and rivers of Albania**

187 The Albanian mountains are parts of the fold belt, which was thrust westward during
188 the subduction of the Adriatic plate beneath southeastern Europe (Roure et al., 2004). The
189 eastern side of Albanides mainly consists of Jurassic ophiolites and Mesozoic carbonates. The
190 western side of Albanides is mainly formed of carbonates topped by Mesozoic or Cenozoic
191 flysch deposits (Robertson and Shallo, 2000). A foreland basin, filled with Plio-Quaternary
192 molasse deposits, forms the coastal plain (Roure et al., 2004).

193 The late Pleistocene uplift rate, inferred from fluvial incision, locally reaches 2.8 mm/yr
194 in the Albanian mountain but is generally in the range 0.5 to 1.0 mm/yr (Carcaillet et al., 2009;
195 Guzmán et al., 2013, Biermanns et al., 2018). Permanent GPS stations indicate the same range
196 of values for the present-day vertical motion in Albania (Jouanne, personal communication).

197 The main Albanian rivers are, from south to north, the Vjosa, Osum, Devoll, Shkumbin,
198 Erzen, Mat and Drin rivers (**Figure 1**) and all of them are less than 272 km long.



199

200 **Figure 2.** Examples of sedimentary units and terraces in Albania. **a)** Remnant of a fill terrace
201 ($T10_{(vj)}$), middle section of the Vjosa River; **b)** Debris flow deposited above $T5_{(vj)}$ terrace

202

203 Fluvial terrace deposition punctuates the vertical incision along all the main Albanian
 204 rivers (**Figure 2**) and most of them are located above soft elastic (flysch or molasses) sediments.
 205 The terraces of the upper Vjosa River (also called Voidomatis in Greece), the middle Vjosa
 206 River, the Osum River, the Erzen River and the Drin River were previously mapped and dated
 207 by Woodward et al. (2008), Hauer et al. (2021), Carcaillet et al., (2009), Koçi (2007) and by
 208 Gemignani et al. (2022), respectively. We performed an analysis of the terrace geometry and
 209 new dating for the Devoll, Skumbin, Mat and Erzen rivers, previously poorly studied. The lower
 210 part of the Drin River has not been studied because it is drowned by several artificial dams.

211

212 4. Terrace geomorphology and ages along the seven Albanian rivers

213 A synthesis of the numerical dating and terrace geometry is presented for the rivers of
 214 Albania and northwestern Greece. A nomenclature is proposed, where the successions of
 215 terraces surface for each river are called $T_{X(\text{river})}$ and terrace indices increase with age. Units are
 216 nonetheless labelled $U_{X(\text{river})}$ when the terrace surface, fully eroded, cannot be defined. A
 217 correlation of this nomenclature with those used by the previous terrace studies is shown in
 218 **Table 3** and detailed in **Supplementary Information, Appendix 3**.

219

River	Middle section	Vjosa upper section	Osum	Palco-Devoll	Erzen	Mat	Drin	Regional nomenclature	Regional abandonment ages (ka)	
Author	<i>P & M, 1987</i> <i>G et al., 2013</i>	<i>Woodward et al., 2008</i> This study	<i>Carcaillet et al., 2009</i> This study	<i>Melo, 1961 - Shkumbin riv.</i> <i>Prifti, 1984 Devoll river</i> This study	<i>Koçi et al., 2018</i> This study	<i>Melo, 1996</i> This study	<i>Gemignani et al., 2022</i> This study			
T e r r a c e	T_I (P & M)	U8	T10(vj)	T10(os)	T12(pa)	-	-	T6(dr)	T12	>350 ?
			T9(vj)	T9(os)	T11(pa)	-	T9(ma)	T5(dr)	T11	>193
					U10(pa)				U10(pa)	
	T_{II} (P & M)	U7	T8(vj)	T8(os)	T8(pa)	T7(er)	T8(ma)		T10	90-117
	T_{III} (P & M)	U6	T7(vj)	-	-	-	T7(ma)		T9	68-87
	T_{II} (P & M)	U5	T6(vj)	T3	T7(os)	T2	T6(ma)		T8	82 (±2-3)
				T4	T6(pa)	T7	T5(ma)		T7	42 (±0.5-1.5)
				T5	pT5(os)	pT6(pa)	T4		T6	35.5 (±1-2)
	T_I (P & M)		T5(vj)	T6	T4(os)	T3	T5(ma)		T5	29.5 (±1)
									T4	16.5-22
			U4	T4(vj)	-	T4(pa)	-	T4(ma)	T3	11-12
			U3	T3(vj)	T7	T3(os)	-	T3(ma)	T2	5.7-6.3; 7.6-10
				T8	T2(os)	-	-	T2(ma)	T1	0.2-1
	T_I (G & al.)	U2	T2(vj)	-	T1	T1	T2(pa)	T1	T0	0-0.2
		U1-actual	T1(vj)	T9	T1(os)	T2(pa)	T5	T1(ma)	T0	0-0.2

220

221 **Table 3.** Correlation of the local terrace nomenclatures with a regional nomenclature for the terraces
 222 identified along the Albanian rivers. The light green cells refer to dated levels; light yellow and white
 223 cells refer to not dated levels, well correlated or poorly correlated, respectively. The colored cells on
 224 the right side refer to the color code of **Figures 3, 5, 7 and 9**. The regional ages of the terrace and their
 225 uncertainties (68% probability interval) are obtained from the probability density curves of the
 226 numerical dating for terraces younger than 60 ka (see text and **Figure 9**). “P & M” stands for Prifti
 227 and Meçaj (1987) and “G and al.” stands for Guzman et al. (2013).

228

229 4.1. Previous studies of the Vjosa, Drin and Osum river terraces

230 The Vjosa River is more than 272 km long and is made up of sections with very different
 231 morphologies (Hauer et al., 2021).

232 In the upper section (Konista area, **Figure 1**), eight units (**Figure 4a**), including the
 233 present-day channel ($T1_{(vj)}$), were identified. They were dated, except $T2_{(vj)}$, using different

234 methods (^{14}C , U/Th, ESR, TL) (Lewin et al., 1991; Hamlin et al., 2000; Woodward et al., 2001;
235 2008) (**Table 2**). The highest terrace was deposited by a river system with a much larger
236 catchment that was pirated before 350 ka (Macklin et al., 1997).

237 In the middle section of the Vjosa River, the long-term incision rate is greater than in
238 the upper section (Guzman et al., 2013). The elevation of the highest terrace T10_(vj) (**Figure 3a**)
239 is more than 160 m (Prifti, 1981) and our field work has shown that the conglomerate unit of
240 T10_(vj) is preserved between paleo-meanders filled by sediment of T9_(vj). Prifti and Meçaj (1987)
241 mapped five terrace levels and Guzman et al. (2013) mapped another terrace level T2_(vj) that is
242 located at the top of a thick sedimentary unit that extends several tens of meters below the
243 present river (Prifti, 1981).

244 The units beneath the terrace surfaces are mainly formed of rounded fluvial clasts.
245 Nonetheless, angular calcareous clasts are locally intercalated within the fluvial units and are
246 related to debris flows (**Figure 3b**) provided by very steep calcareous slopes. Guzman et al.
247 (2013) dated colluvium above the top of T2_(vj).

248 We dated in this paper T5_(vj) with an age intercalated between those found in the upper section
249 for T4_(vj) and T6_(vj) (Woodward et al., 2008). Hence, when the upper and middle sections of the
250 Vjosa River are considered, ten river terrace levels are identified and only T9_(vj) is not dated
251 (**Figure 3a, Table 2**).

252 Along the Drin River, four terraces are described (Aliaj et al., 1996; Pashko and Aliaj,
253 2020). Our personal work close to Peshkopia area (**Figure 1**) has revealed two others higher
254 terraces, T5_(dr) and T6_(dr) (**Figure 3f**). Only T2_(dr) and T3_(dr) terraces were dated (Gemignani et
255 al., 2022) (**Table 2**).

256 In the Osum River area, nine terraces were mapped (Carcaillet et al., 2009) and our
257 complementary observations indicate remnants of a fill terrace (T10_(os)) more than 150 m above
258 the present-day river (**Figure 3b**). The sedimentary unit linked to T4_(os) is superimposed above
259 another allostatigraphic unit U5_(os) in the middle reaches of the Osum River (Carcaillet et al.,
260 2009). Using ^{14}C and ^{10}Be dating methods, Carcaillet et al. (2009) dated T7_(os), T6_(os), T3_(os),
261 and T2_(os) and also U5_(os) (**Table 2**).

262
263
264
265
266
267

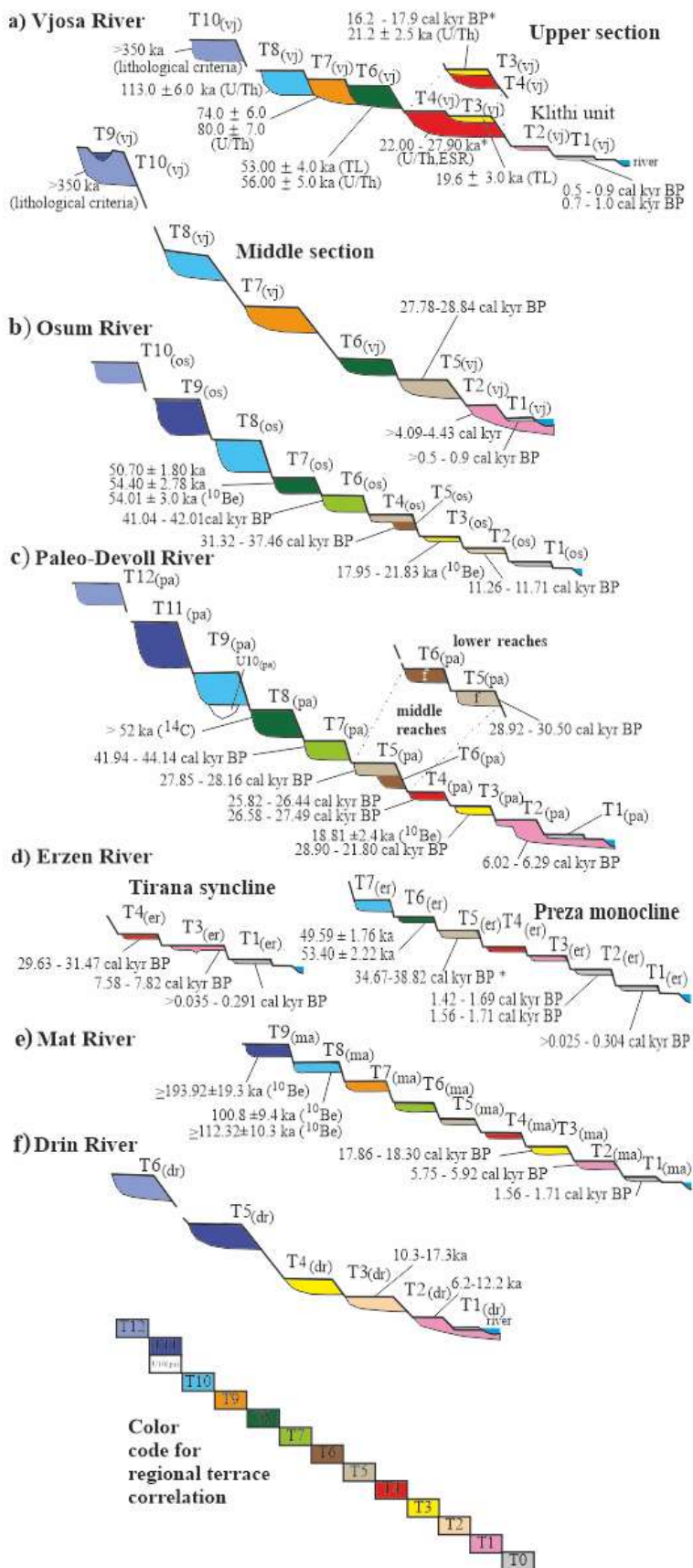


Figure 3. Ages and simplified geometry of the terraces identified along the 7 main Albanian rivers (a to f; see text). The horizontal and vertical axes are not to scale. The local terrace nomenclature TX_(loc) is indicated for each river. The color of the terraces indicates the inferred correlation with the regional nomenclature T0 to T12 (Same colors as cells of Table 3). The ages refer to the numerical ages of Table 2. Ages are shown as a unique interval with an “*” if there are three or more numeric dates for one terrace level.

304 **4.2 New results about the paleo-Devoll, Mat and Erzen terraces**

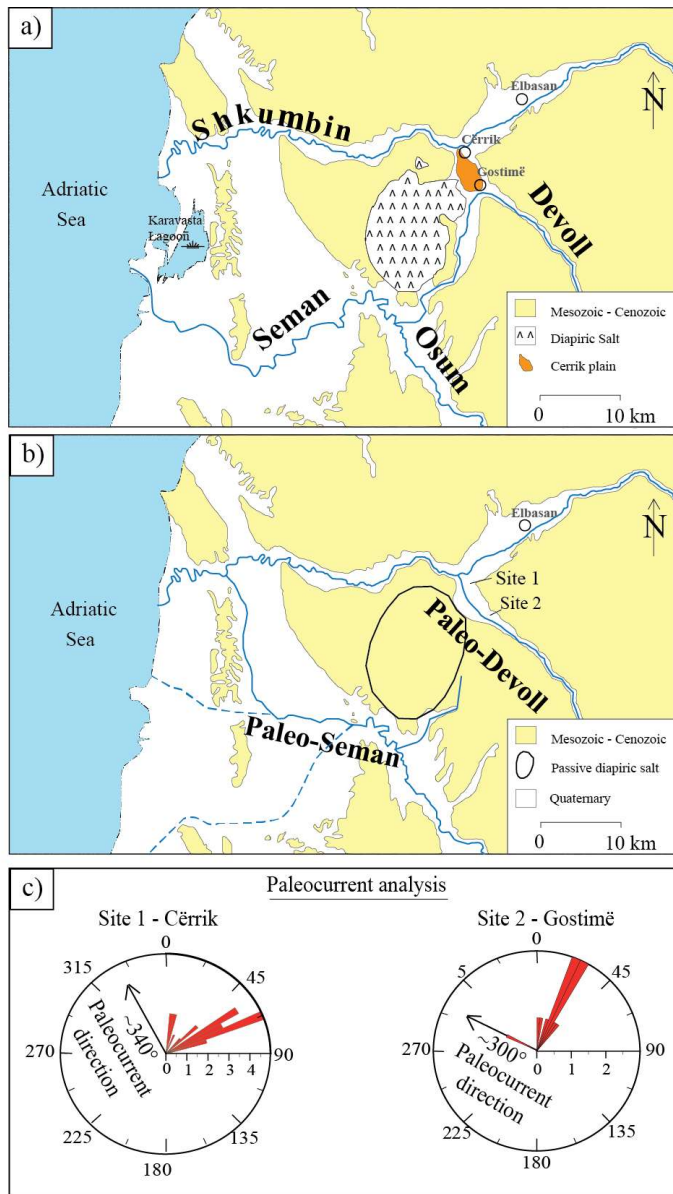
305

306 **4.2.1. A paleo-Devoll River defined from the Devoll and Shkumbin terraces**

307 The Devoll River flows over 205 km. Downstream from the confluence with the Osum

308 River, it forms the Seman River (**Figure 5a**).

309



310

311 **Figure 4.** Evolution of the connections between the Devoll, Osum, Seman and Shkumbin rivers. **a)**

312 *Present-day configuration. b) Previous configurations. The age of the capture of the Devoll by the*

313 *Seman is estimated at 6 ka (see text). The paleo-Seman River from Chabreyrou (2006; full line) and*

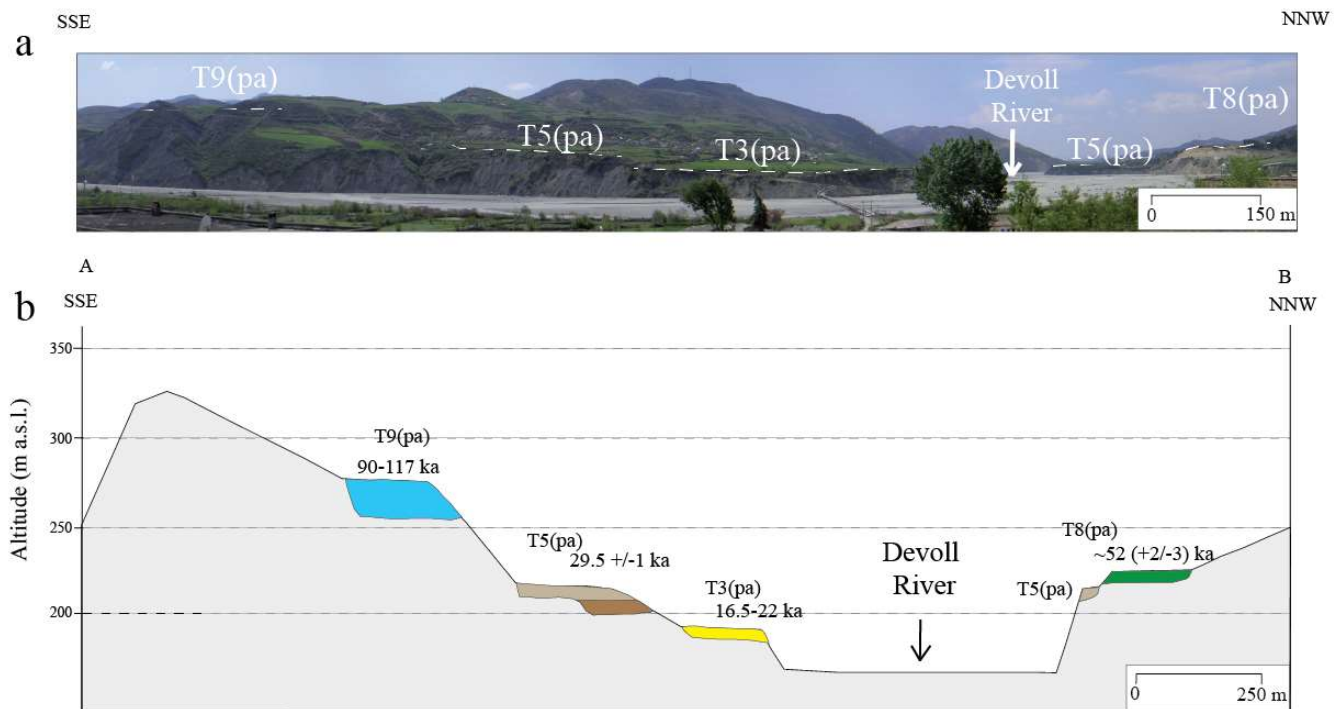
314 *Fouache et al (2010; dashed lines). c) Rose diagrams of the paleo-flow directions inferred from*

315 *imbricate clasts and cross stratification. Location of sites 1 and 2 on **Figure 4b** (data in the*

316 **Supplementary Information Appendix 4).**

317 The Shkumbin River is 181 km long and the Devoll and Shkumbin are two nearby rivers
 318 that are presently separated by the Cërrik plain spanning approximately 20 km². Today, no river
 319 flows through this plain (**Figure 5a**) that dips ~0.1° toward the northwest but terraces of a paleo-
 320 river are perched above its eastern border. The Cërrik plain is located over a thick sedimentary
 321 unit (Prifti and Meçaj, 1987) and the scarp cut by the Devoll River shows a > 12 m-thick deposit
 322 formed of pebbles supported by a sandy to silty matrix. Our measurements of imbricate clasts
 323 and cross stratification indicate paleo-flow directions around N 300° and N 340° during
 324 deposition (site 1 and 2 on **Figure 4c** and **Supplementary Information Appendix 4**). This
 325 suggests that the paleo-Devoll River flowed northward and connected to the Shkumbin River.
 326 Hence, the terraces located along the middle reaches of the Devoll and the lower reaches of the
 327 Shkumbin form a unique terrace system that extends more than 100 km.

328 Four and six terrace levels were initially identified along the Shkumbin (Melo, 1961)
 329 and Devoll (Prifti, 1984) rivers, respectively. In this study (**Supplementary Information**
 330 **Appendix 5**), we mapped and correlated eleven terrace levels along the paleo-Devoll River
 331 (**Table 3** and **Figure 3c**). Their sedimentary units were generally deposited on straths beveled
 332 in the flysch or molasse substratum.



334 **Figure 5.** The terraces of the upper reaches of the Devoll River. **a)** Panoramic view and **b)** cross-section
 335 through the terraces. The ages refer to the regional nomenclature and to the most likely age of
 336 abandonment proposed in this study (**Table 3**).

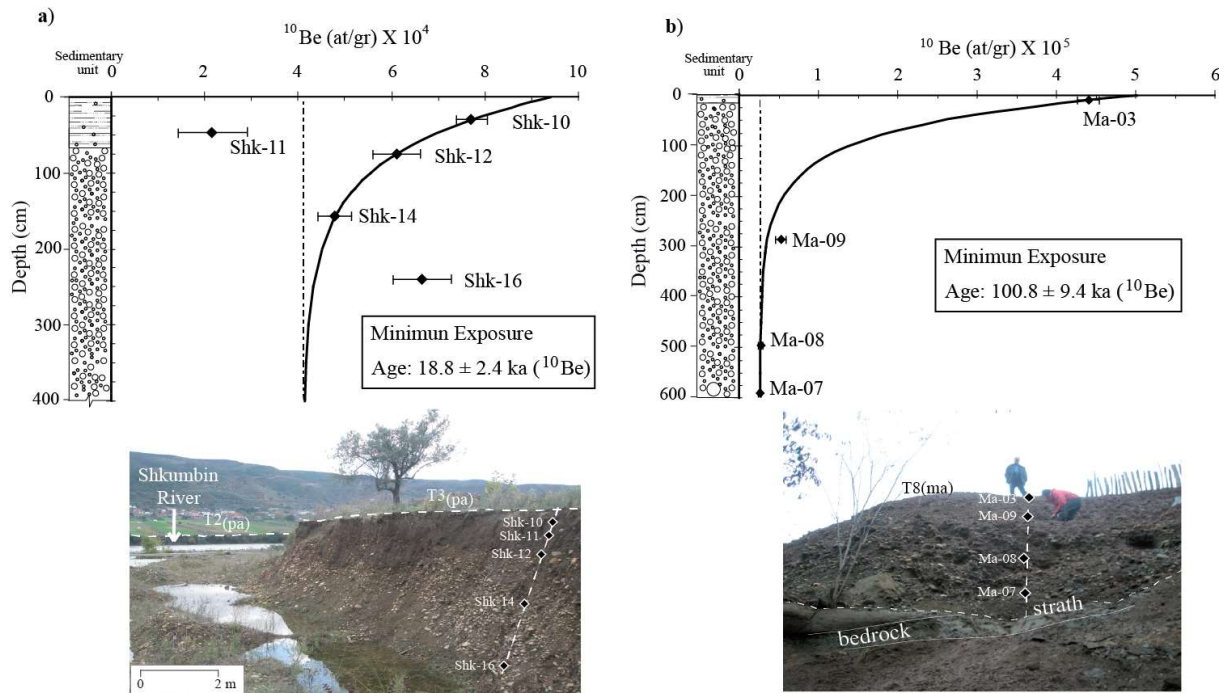
337

338 The mean thickness of T12_(pa), T11_(pa), T9_(pa), T8_(pa), T7_(pa), pT6_(pa), and T5_(pa), T4_(pa) and
339 T3_(pa) vary between 6 and 32 m and two superposed sub-units, that are part of parts of the same
340 fluvial process, are found beneath all these terraces: A thin upper sedimentary sub-unit (~1 m)
341 is composed of clay, siltstone and fine sand. Nevertheless, its thickness reaches more than 2 m
342 beneath the oldest terraces (T12_(pa), T11_(pa) and T9_(pa)) and possibly includes loess and colluvium
343 deposited after the fluvial story. The basal sub-unit consists of rounded pebbles and cobbles
344 that are supported by a gravel and sand matrix. The clast size generally fines upward, while the
345 percentage of matrix increases. Nonetheless, the size of the coarse material shows complex
346 variations and conglomerate sometimes alternate with horizontal stratified, fine to coarse sand
347 levels. Sediments of the basal unit were deposited in a braided alluvial system characterized by
348 cross-stratified rounded pebbles and cobble levels that alternate with horizontal stratified, fine
349 to coarse sand levels.

350 The upper part of T10_(pa) is fully eroded and U10_(pa) is only found beneath an erosional
351 surface in the continuity of the strath at the bottom of T9_(pa). Evidence of a meandering
352 environment is found within the unit U10_(pa) (**Figure 3c**) where sediments dip steeply and were
353 possibly deposited at the intrados of meanders.

354 In the lower reaches of the paleo-Devoll catchment, a cosmogenic depth profile (**Figure**
355 **8a**) yielded a minimum exposure age for T3_(pa) (**Table 1**; see the description in **Supplementary**
356 **Information, Appendix 2**) and seven ¹⁴C samples were collected along the paleo-Devoll River
357 (**Table 2**). These results, combined with the eleven ¹⁴C dates (Guzmán et al., 2013) gave ages
358 for T8_(pa), T7_(pa), T5_(pa), T4_(pa), T3_(pa), and T2_(pa). Furthermore, the ¹⁴C dating of colluvium
359 deposited above T1_(pa) provides an age for the abandonment of this terrace.

360

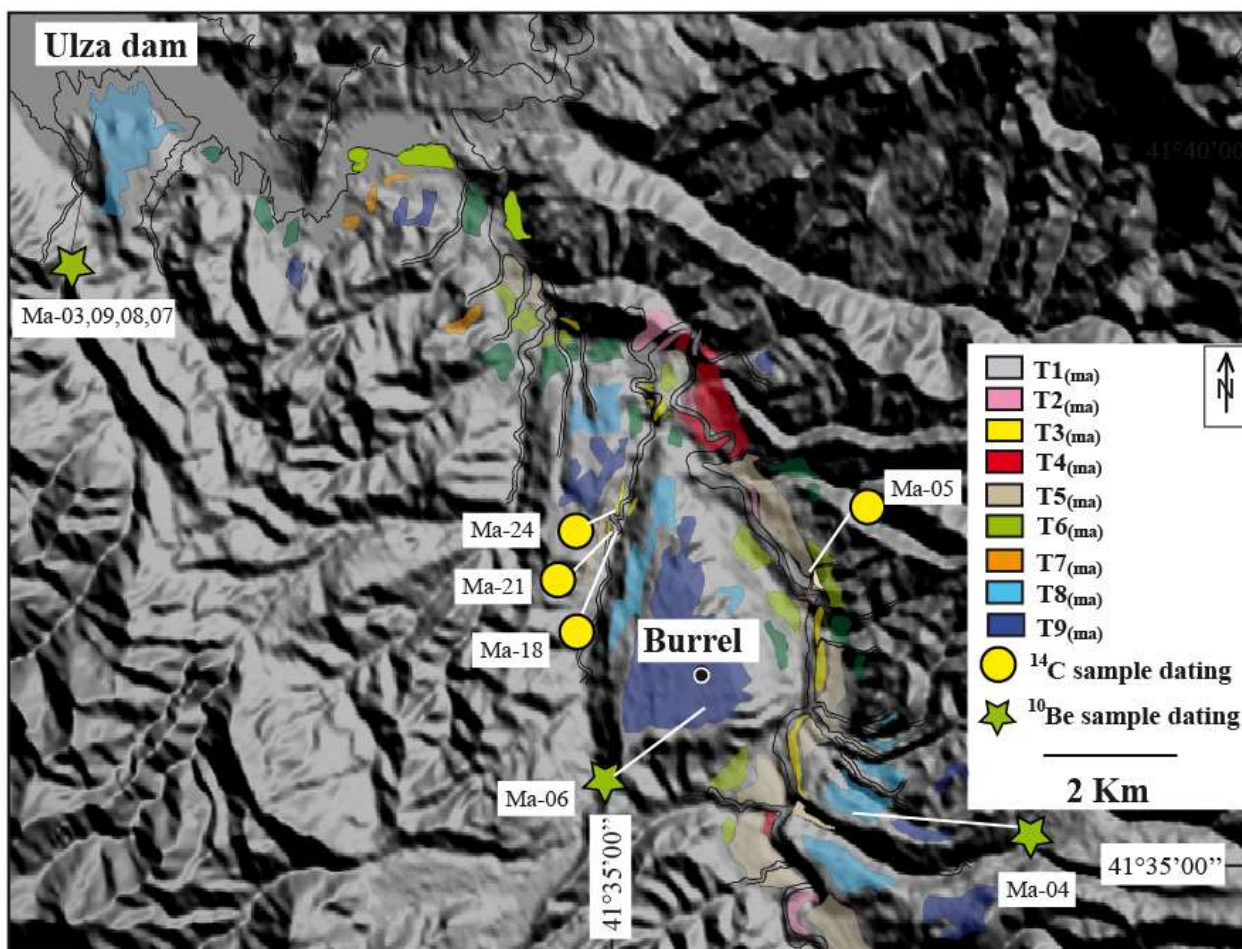


361
 362 **Figure 6.** The ^{10}Be concentration along the depth profiles. **a)** T3_(pa) in the lower reaches of the paleo-
 363 Devoll River (location of Sk-10 on the **Supplementary Information, Appendix 5a**); **b)** T8_(ma) in the
 364 middle reaches of the Mat River (Ulza Dam, location on **Figure 7**). Solid lines indicate the best-fit for
 365 the depth-production profile; the dashed line shows the inherited ^{10}Be concentration. Details are given
 366 in **Table 1** and in the **Supplementary Information Appendix 2**.

4.2.2 Characteristics and numerical ages of the Mat terraces

368 Five terraces were previously described along the Mat River (Melo, 1996). Nine terraces
 369 (**Figure 3e**) were mapped during our fieldwork (**Figure 7**).

371 The two oldest terraces were dated using the ^{10}Be method. Amalgams of siliceous
 372 pebbles (e.g. radiolarites, chert, quartz), were taken at the top of T9_(ma) and T8_(ma) (Ma-06 and
 373 Ma-04 in **Table 1**; location on **Figure 7**). A cosmogenic depth profile was made through the
 374 sedimentary unit of terrace T8_(ma) (**Figure 6b**). Terraces T3_(ma), T2_(ma), T1_(ma) and the colluvium
 375 deposited above T1_(ma) were dated from charcoal samples (**Table 2** and **Figure 3e**).



378
 379 **Figure 7:** Geomorphologic map of the Mat River. Location on **Figure 1**. The numbers refer to
 380 the samples of **Table 2**.

381
 382 **4.2.3. Characteristics and numerical ages of the Erzen terraces**

383 The terraces of the Erzen River have been mapped by Koçi (2007) and an active back-
 384 thrust fault separates two domains (Ganas et al., 2020). In the western uplifted domain (Prespa
 385 monocline), seven levels of terraces were recognized (**Figure 3d**) whereas in the eastern domain
 386 (Tirana syncline), only three terrace levels were recognized. A correlation between the terraces
 387 on each side of the back-thrust fault is made using the 15 ¹⁴C dates (**Table 2**) and seven terrace
 388 levels were identified along the Erzen River (T7_(er) to T1_(er)), and only the oldest level is not
 389 numerically dated. The terrace T3_(er) is highly extended, in peculiar across a wind gap (**Figure**
 390 **8**), which corresponds to a paleo river that flowed close to Tirana (**Figure 1**).

391



392

393 **Figure 8.** Terraces of the Erzen River. ($T3_{(er)}$) extending toward the Tirana wind gap.

394

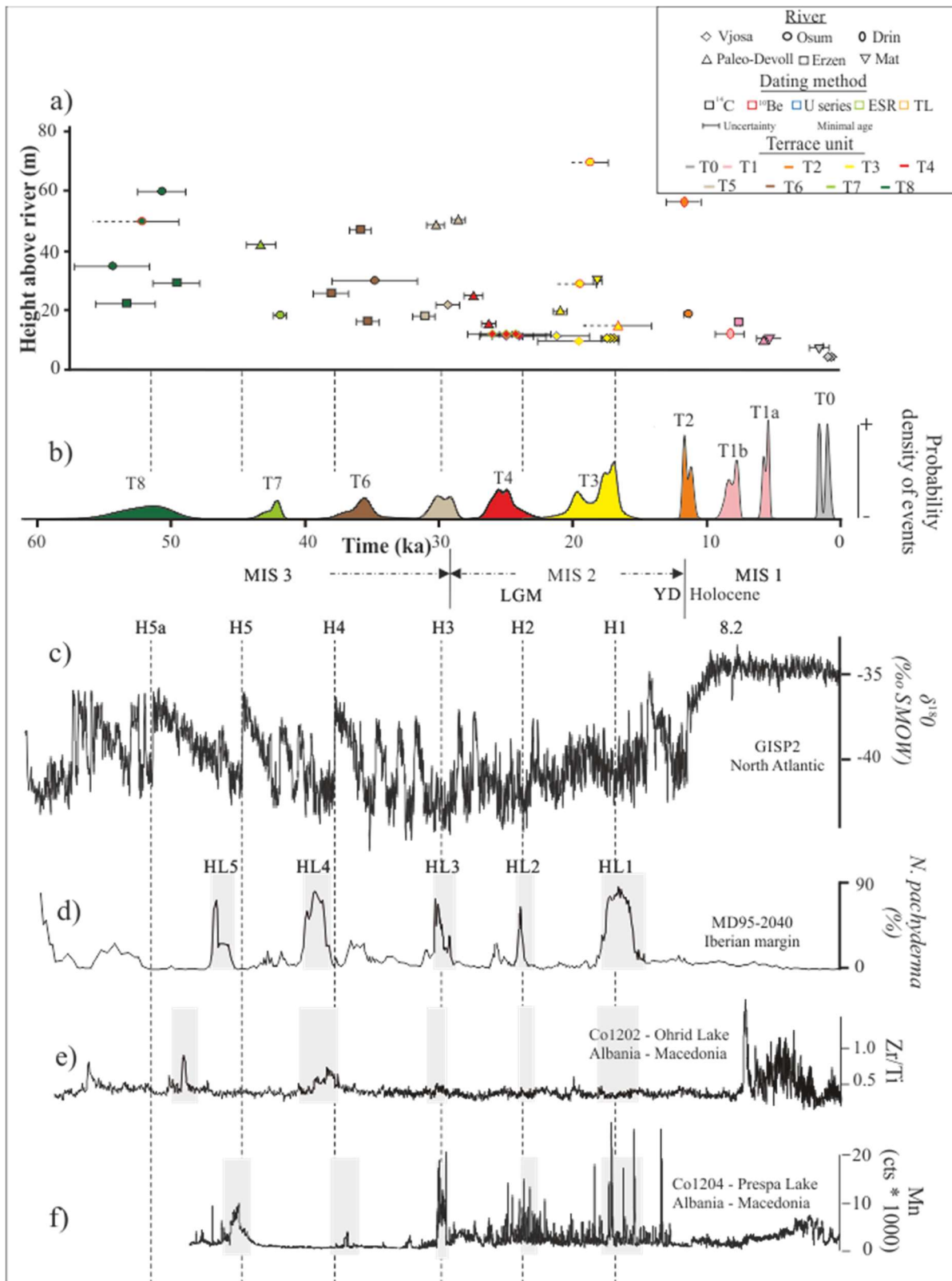
395 5. Discussion

396 5.1 A regional correlation of the Albanian terraces based on numerical ages

397 Few samples have been discarded during our work (**Table 2**): two ^{14}C samples, that
398 furnished less than 200-year ages in old terraces, were considered as related to the reworking
399 of recent organic pieces. The Carbon quantity of five samples was too small (less than 0.12 mg)
400 to give numerical ages. Two ^{10}Be samples were also excluded from the profile interpretations
401 because one was probably transported by a small tributary and the other one affected by a
402 probable chemical problem during the preparation (**Supplementary Information, Appendix**
403 **2**). Finally, two TL ages published by Lewin et al. (1991) were removed due to their very high
404 uncertainty.

405 Thirty-one out of the 49 local terrace levels ($\text{Tx}_{(\text{river})}$, **Figure 4**) recognized along the
406 seven rivers were dated, providing a solid framework for a regional correlation (Tx) based on
407 the synchronicity of numerical ages. No simple relationship between altitude and age is
408 observed at the scale of Albania (**Figure 9a**) due to the variable uplift rate in the Albanian
409 mountains (Guzman et al., 2013).

410 To consider the 60 numerical ages younger than 60 ka, a regional probability density
411 curve was obtained from the summation of the individual probability distribution ages (Ramsey,
412 2009), a method already used in terrace chronology studies (e.g. Meyer et al., 1995; Wegmann
413 and Pazzaglia, 2002; 2009). The summation (**Figure 9b**) shows time periods where the
414 probability of sedimentation is null and ten high probability peaks. These peaks define the ages
415 of T0 to T8 (**Table 3**, see details of the correlation in **Supplementary Information, Appendix**
416 **6**).
417



418
 419 **Figure 9.** Compilation of the Albanian terrace ages for the last 60 ka (**Table 2**) and comparison
 420 with climatic proxies. **a)** Plot of individual ages and their two sigma (95%) probability. Each terrace is
 421 represented by a symbol, a contour color and a fill color corresponding to the river, the dating method
 422 and the terrace level (regional nomenclature), respectively. The horizontal axis is the terrace age while
 423 the vertical axis is the height of the terrace above the present-day river. **b)** The regional probability

424 density curve produced by summing the probability distribution of the individual ages; c) The $\delta^{18}O$
425 record from the GISP2 ice core (Grootes et al., 1993). d) The percentage of the cold-water foraminifera
426 *N. pachyderma* from the Iberian margin (de Abreu et al., 2003); e) The paleo-environmental record
427 from Lake Ohrid (Zirconium/Titanium ratio: Zi/Ti) (Wagner et al., 2009); and f) the paleo-
428 environmental record from Lake Prespa (Manganese: Mn) (Wagner et al., 2010). The timings of the
429 Heinrich events (H1 to H5a) are taken from Rashid et al. (2003) and Hemming (2004). The gray
430 rectangles represent the Heinrich events as identified by the authors of curves d, e, f. MIS, LGM and
431 YD stand for Marine Isotope Stage (Cacho et al., 1999), Last Glacial Maximum (Clark et al., 2009) and
432 Younger Dryas (Berger, 1990), respectively.

433

434 The ages greater than 60 ka are few in number and the regional T9 to T12 levels are
435 only defined by one or two ages. Eighteen terrace levels are not numerically dated along the
436 various rivers. Their intercalation between dated levels provides a rather good relative age
437 (yellow cells on **Table 3**) or their elevation relative to the dated terrace levels only provides a
438 poor relative chronology (white cells in **Table 3**).

439

440 **5.2. The influence of the paleoclimate on the genesis of Albanian terraces**

441 The comparison of the Albanian terraces ages with climatic proxies (Grootes et al.,
442 1993; de Abreu et al., 2003; Wagner et al., 2009, 2010) is a rather difficult exercise given the
443 uncertainties about the terrace abandonment ages (more than one thousand years) and the short-
444 term fluctuations in the climatic records (less than one thousand years, Ziemmen et al., 2018). A
445 robust criterion could be based on models that link the timing of sedimentation and incision
446 with the temperature, hydrology and vegetation evolutions during a climatic cycle (Bull, 1991).

447 Cold periods in Albania are associated with less precipitation (Kallel et al., 2000;
448 Toucanne et al., 2015) and we consider the classic model for these climatic contexts, where
449 vertical incision is favored by the increase of the transport capacity that occurs at the transition
450 from cold and dry conditions to warmer and more humid conditions (e.g. Fuller et al., 1998;
451 Bridgland and Westaway, 2008). This model has been proposed to define the “cold” terraces in
452 the lowlands of northern Europe (Vandenbergh, 2015), to correlate terraces at the
453 Mediterranean scale (Macklin et al., 2002), to interpret terraces in semi-arid conditions
454 (Vassallo et al., 2007) and to interpret the nested terraces in Northern Apennines (Wegmann
455 and Pazzaglia, 2009) or the western Carpathians (Olszak, 2017).

456 The succession of cold periods followed by rapid warm excursions, could effectively
457 cause the abandonment of most terraces (**Figure 9c**): T2, T6 and T7 are synchronous with the

458 end of the Younger Dryas, the Dansgaard-Oeschger events number 7 and 11, respectively
459 (Dansgaard et al., 1993; North Greenland Ice Core Project Members, 2004). Furthermore, the
460 abandonments of T8, T5, T4, and T3 (**Figure 9b**) correlate rather well with the H5a (Rashid et
461 al., 2003), H3, H2, and H1 Heinrich events (Hemming, 2004), respectively (**Figure 9c**). These
462 Heinrich events were already recorded in this area (Wagner et al., 2009; 2010) (gray rectangle
463 on **Figures 11d, e and f**).

464 The ranges of the terrace ages, defined by the 95% probability interval of the summation
465 curve, therefore include the ages of transitions between cold-dry and warm-wet periods.
466 Nonetheless, as the climatic transitions were dated more precisely than the Albanian terraces
467 (less than a thousand years vs. more than a thousand years), our results do not prove the "cold"
468 terrace model of Vandenberghe (2008) and are only in agreement with this model of terrace
469 genesis.

470 However, while rapid changes during the glacial cycle, such as DO or HE events, can
471 induce the formation of "cold" terraces, the major changes that occur between the glacial and
472 interglacial periods are not generally considered in this model. This is the case of T1 that is not
473 synchronous with a cold to warm transition. Vandenberghe (2008) suggests that, in addition to
474 the "cold" terrace model, deep channels may be very rapidly incised and then filled at the
475 beginning of a warm period. This results in a "warm" unit model (Vandenberghe, 2008) and
476 situations of rivers leaving their valley to take another course (Vandenberghe, 1993) frequently
477 typify "warm" units (Vandenberghe, 2015).

478 T1 is related to the Holocene climatic optimum and a great aggradation along the Vjose
479 (**Figure 3a**) as well as deviations of the rivers at the Cërrik and the Tirana wind gaps (**Figure**
480 **4 and Figure 8**) were recorded during this period. The T1 terrace would therefore be in line
481 with the "warm" unit model (Vandenberghe (2015). Similarly, the U10_(pa), remnant of a valley
482 fill older than the T10 (90-117 ka) overlying unit, may have been deposited during the Eemian
483 interglacial (MIS-5e) stage and could be a "warm" sedimentary unit (Vandenberghe, 2015).

484

485

486

487

488 **6. Conclusions**

489 Geomorphologic studies and new dating have been performed along the Devoll,
490 Shkumbin, Mat and Erzen rivers of Albania (30 ¹⁴C sites, two ¹⁰Be profiles and two ¹⁰Be surface
491 sites). A comparison is also made with previous studies along the Vjosa, Osum and Drin rivers.

492 This work has led to a database of 70 ages and a time correlation has been performed between
493 the flights of terraces observed along the seven rivers. It appears that 11 terrace levels have
494 been preserved during the last 200 ka in Albania and this record contains most of the major
495 phases of terrace formation in the Mediterranean region during the last glacial cycle. The
496 exceptional preservation of the succession of Albanian terraces is probably due to the
497 combination of a moderate uplift rate (0.5 to 1 mm/year) and a medium strength of the bedrock
498 lithology (mainly flysch or molasse) specific to this area. During the Holocene, T1 terrace level
499 was recognized, along with the capture of the Devoll River by the Osum River and a tributary
500 deviation away from the Erzen. Eight terraces (T2 to T10) were identified and dated during the
501 last glacial period (MIS 5d to end of MIS 2). For the older periods, a unique terrace remnant of
502 T11 was dated at $\geq 194 \pm 19$ ka (MIS 6).

503 The abandonment of the Albanian terrace surfaces was mainly controlled by climatic
504 variations and was generally synchronous with the interstadial transitions during the last glacial
505 period. This indicates that the threshold necessary for a cold to warmer climatic control for
506 terrace development is reached during interstadial climatic events as short as Heinrich events.

507

508 **Supplementary Information**

509 APPENDIX 1 Technical details for ^{14}C dating and location of the samples.

510 APPENDIX 2. Technical details for ^{10}Be dating and description of the attenuation profiles.

511 APPENDIX 3. Correlation of terraces defined in previous studies of the Vjosa River.

512 APPENDIX 4. Paleo-current data from the Gostimë-Cërrik plain.

513 APPENDIX 5. Geomorphologic maps of the Paleo-Devoll River

514 APPENDIX 6. Determination of regional terrace levels from a time correlation

515

516 **Acknowledgements**

517 The authors would like to thank the NATO SFP 977993 and the Science for Peace team for
518 supporting this work. OG thanks the Simon Bolivar University for granting him permission to
519 carry out his doctoral studies. This publication was also made possible through a grant provided
520 by the Institut de Recherche et Developement. We warmly thank the staff of the AMS facility
521 ASTER at the Centre Européen de Recherche et d'Enseignement des Géosciences de
522 l'Environnement (CNRS, France) for technical assistance during the ^{10}Be measurements. We
523 thank one anonymous reviewer and Johannes Preuss for helpful comments.

524

525 **Declaration of interests**

526 "The authors do not work for, advise, own shares in, or receive funds from any organization
527 that would benefit from this article, and have declared no affiliations other than their research
528 organizations."

529 **References**

530 (The references of the supplementary information are included in this list)

- 531
- 532 Aliaj, S., Melo, V., Hyseni, A., Skrami, J., Mëhillka, Ll. Muço, B., Sulstarova, E., Prifti, K., Pashko, P., Prillo, S.,
533 1996. Neo-tectonic map of Albania in scale 1:200000. Edited by Archive of Seismology Institute, Tirana,
534 Albania. (In Albanian).
- 535 Antoine, P., Moncel, M.-H., Limondin-Lozouet, N., Lochet, J., Bahain, J., Moreno, D., Voinchet, P., Auguste, P.,
536 Stoetzel, E., Dabkowski, J., Bello, S., Parfitt, S., Tombret, O., Hardy, B., 2016. Palaeoenvironment and
537 dating of the Early Acheulean localities from the Somme River basin (Northern France): New discoveries
538 from the High Terrace at Abbeville-Carrière Carpentier. *Quaternary Science Reviews*, 149, 338-371,
539 <https://www.sciencedirect.com/science/article/abs/pii/S027379116302700>
- 540 Arnold, M., Merchel, S., Bourles, D., Braucher, R., Benedetti, L., Finkel, R.C., Aumaitre, G., Gott dang, A., Klein,
541 M., 2010. The French accelerator mass spectrometry facility ASTER: Improved performance and
542 developments. *Nucl. Instrum. Methods Phys. Res. B* 268, 1954-1959.
543 <https://www.sciencedirect.com/science/article/abs/pii/S0168583X10002028>
- 544 Bard, E., Rostek, F., Ménot-Combes, G., 2004. Radiocarbon calibration beyond 20,000 14C yr BP by means of
545 planktonic foraminifera of the Iberian Margin. *Quat. Res.* 61, 204-214.
546 <https://www.sciencedirect.com/science/article/abs/pii/S0033589403001698>
- 547 Berger, W. H., 1990. The Younger Dryas cold spell – a quest for causes. *Glob. and Planet. Change* 3 (3). 219–
548 237. <https://www.sciencedirect.com/science/article/abs/pii/0921818190900188>
- 549 Biermanns P., Schmitz B., Ustaszewski K., Reicherter K., 2018. Tectonic geomorphology and Quaternary
550 landscape development in the Albania - Montenegro border region: An inventory. *Geomorphol.*
551 <https://doi.org/10.1016/j.geomorph.2018.09.014>
- 552 Bond, G., Heinrich, H., Broecker, W., Labeyrie, L., Mcmanus, J., Andrews, J., Huon, S., Jantschik, R., Clasen, S.,
553 Simet, C., 1992. Evidence for massive discharges of icebergs into the North Atlantic Ocean during the
554 last glacial period. *Nature* 360, 245-249. <https://www.nature.com/articles/360245a0>
- 555 Braucher, R., Brown, E.T., Bourlès, D.L. Colin, F., 2003. In situ produced ¹⁰Be measurements at great depths:
556 implications for production rates by fast muons. *Earth Planet. Sci. Lett.* 211, 251-258.
557 [https://doi.org/10.1016/S0012-821X\(03\)00205-X](https://doi.org/10.1016/S0012-821X(03)00205-X)
- 558 Bridgland, D., Westaway, R., 2008. Climatically controlled river terrace staircases: A worldwide Quaternary
559 phenomenon. *Geomorphol.* 98, 285-315.
560 <https://www.sciencedirect.com/science/article/abs/pii/S0169555X0700236X>
- 561 Brown, E.T., Edmond, J.M., Raisbeck, G.M. Yiou F., Kurtz M.D., Brook E.J., 1991. Examination of surface
562 exposure ages of moraines in Arena Valley, Antarctica, using *in situ* produced ¹⁰Be and ²⁶Al. *Geochim.*
563 *Cosmochim. Acta* 55, 2269-2283. [10.1016/0016-7037\(91\)90103-C](https://doi.org/10.1016/0016-7037(91)90103-C)bbbb
- 564 Bull, W.B., 1991. *Geomorphic responses to climate change.* Oxford University Press, Oxford, p. 326.
565 <https://www.osti.gov/biblio/5603696>
- 566 Cacho, I., Grimalt, J.O., Pelejero, C., Canals, M., Sierro, F.J., Flores, J.A., Shackleton, N. J., 1999. Dansgaard–
567 Oeschger and Heinrich event imprints in Alboran Sea paleotemperatures. *Paleoceanography* 14, 698-705.
568 <https://www.semanticscholar.org/paper/Dansgaard%E2%80%90Oeschger-and-Heinrich-event-imprints-in-Cacho-Grimalt/a2dda1e4955c28de37c151ae3f0a1fa3400b3ff8>
- 569
- 570 Carcaillet, J., Mugnier, J.L., Koçi, R., Jouanne, F., 2009. Uplift and active tectonics of southern Albania inferred
571 from incision of alluvial terraces. *Quat. Res.* 71, 465-476.
572 <https://www.sciencedirect.com/science/article/abs/pii/S0033589409000039>
- 573 Chabreyrou, J., 2006. Morphologie fluviale et structures tectoniques actives en Albanie. Masters Thesis, Université
574 Joseph Fourier, France.
- 575 Chappell, J., 2002. Sea level changes forced ice breakouts in the Last Glacial cycle: new results from coral terraces.
576 *Quaternary Science Review*, 21, 1229-1240.
577 <https://www.sciencedirect.com/science/article/abs/pii/S027379110100141X>
- 578 Chmeleff, J., Von Blanckenburg, F., Kossert, K., Jakob, D., 2010. Determination of the ¹⁰Be half-life by
579 multicollector ICP-MS and liquid scintillation counting. *Nucl. Instrum. Methods Phys. Res.* 268, 192-
580 199. Chmeleff, J., Von Blanckenburg, F., Kossert, K., Jakob, D., 2010. Determination of the ¹⁰Be half-
581 life by multicollector ICP-MS and liquid scintillation counting. *Nucl. Instrum. Methods Phys. Res.* 268,
582 192-199. <https://www.sciencedirect.com/science/article/abs/pii/S0168583X09009793?via%3Dihub>
- 583 Clark, P. U., Dyke, A. S., Shakun, J. D., Carlson, A.E., Clark, J., Wohlfarth, B., Mitrovica, J. X., Hostetler, S. W.,
584 2009. The last glacial maximum. *Science* 325, 710-714.
585 <https://www.science.org/doi/10.1126/science.1172873>
- 586 Clement, A. C., Peterson, L. C., 2008. Mechanisms of abrupt climate change of the last glacial period, *Rev.*
587 *Geophys.* 46, RG4002, <https://doi.org/10.1029/2006RG000204>

- 588 Cordier, S., Briant, B., Bridgland, D., Herget, J., Maddy, D., Mather, A., Vandenberghe, J., 2017. The Fluvial
589 Archives Group: 20 years of research connecting fluvial geomorphology and palaeoenvironments.
590 Quaternary Science Reviews 166, 1-9.
591 <https://www.sciencedirect.com/science/article/abs/pii/S0277379117301944>
- 592 Cremaschi, M., Zerboni, A., Nicosia, C., Negrino, F., Rodnight, H., Spötl, C., 2015. Age, soil-forming processes,
593 and archaeology of the loess deposits at the Apennine margin of the Po plain (northern Italy): New
594 insights from the Ghiardo area. Quaternary International, 376, pp. 173-188.
595 <https://www.sciencedirect.com/science/article/abs/pii/S1040618214005138>
- 596 Dansgaard, W., Johnsen, S. J., Clausen, H. B., Dahl-Jensen, D., Gundestrup, N. S., Hammer, C. U., Hvidberg, C.
597 S., Steffensen, J. P., Sveinbjörnsdóttir, A. E., Jouzel, J., Bond, G. 1993. Evidence for general instability
598 of past climate from a 250,000- year ice-core record. Nature 364, 218-220.
599 <https://www.nature.com/articles/364218a0>
- 600 de Abreu, L., Shackleton, N. J., Schönfeld, J., Hall, M. A., Chapman, M.R., 2003. Millennial-scale oceanic climate
601 variability off the Western Iberian margin during the last two glacial periods. Mar. Geol. 196, 1-20.
602 <https://www.sciencedirect.com/science/article/abs/pii/S002532270300046X>
- 603 Dunne, J., Elmore, D., Muzikar, P., 1999. Scaling factors for the rates of production of cosmogenic nuclides for
604 geometric shielding and attenuation at depth on sloped surfaces. Geomorphology 27, 3-11.
605 <https://www.sciencedirect.com/science/article/abs/pii/S0169555X98000865>
- 606 Fouache, E., Vella, C., Dimo, L., Gruda, G., Mugnier, J-L, Deneffe, M., Monnier, O., Hotyat, M., Huth, E., 2010.
607 Shoreline reconstruction since the Middle Holocene in the vicinity of the ancient city of Apollonia
608 (Albania, Seman and Vjosa deltas). Quaternary International, 216, 118-128.
609 <https://doi.org/10.1016/j.quaint.2009.06.021>
- 610 Fuller, I.C., Macklin, M.G., Lewin, J., Passmore, D.G., Wintle, A.G., 1998. River response to high-frequency
611 climate oscillations in southern Europe over the Past 200 k.y. Geology 26, 275-278.
612 [https://www.researchgate.net/publication/249520546_River_response_to_high-](https://www.researchgate.net/publication/249520546_River_response_to_high-frequency_climate_oscillations_in_southern_Europe_over_the_past_200_ky)
613 [frequency_climate_oscillations_in_southern_Europe_over_the_past_200_ky](https://www.researchgate.net/publication/249520546_River_response_to_high-frequency_climate_oscillations_in_southern_Europe_over_the_past_200_ky)
- 614 Ganas, A., Elias, P., Briole, P., Cannavo, F., Valkaniotis, S., Tsironi, V., Partheniou, E., 2020, Ground Deformation
615 and Seismic Fault Model of the M6.4 Durres (Albania) Nov. 26, 2019 Earthquake, Based on NSS/INSAR
616 Observations. Geosciences, 10, 210; [doi:10.3390/geosciences10060210](https://doi.org/10.3390/geosciences10060210)
- 617 Gemignani, L., Mittelbach, B., Simon, D., Rohrmann, A., Grund, M., Bernhardt, A., Hippe K., Giese J., Handy,
618 M., 2022. Response of Drainage Pattern and Basin Evolution to Tectonic and Climatic Changes Along
619 the Dinarides-Hellenides Orogen. Front. Earth Sci. 10:821707. [doi: 10.3389/feart.2022.821707](https://doi.org/10.3389/feart.2022.821707)
- 620 Geraga, M., Tsaila-Monopolis, S., Ioakim, C., Papatheodorou, G., Ferentinos, G., 2005. Short-term changes in
621 the southern Aegean Sea over the last 48,000 years. Palaeoceanol. Palaeoclimatol. Palaeoecol. 220,
622 311-332. <https://www.sciencedirect.com/science/article/abs/pii/S0031018205000428>
- 623 Gosse, J., Phillips, F., 2001. Terrestrial in situ cosmogenic nuclides: theory and application. Quat. Sci. Rev. 20,
624 1475-1560. <https://www.sciencedirect.com/science/article/abs/pii/S0277379100001712>
- 625 Grootes, P. M., Stuiver, M., White, J., Johnson S., Jouzel, J., 1993. Comparison of oxygen isotope records from
626 the GISP2 and GRIP Greenland ice cores. Nature 366, 552-554.
627 <https://www.nature.com/articles/366552a0>
- 628 Guzmán, O., Mugnier, J.L., Vassallo, Koçi, R., Jouanne, F., 2013. Vertical slip rate of major active faults of
629 southern Albania inferred from river terraces. Annals Geophys. Earthquake Geol. 56, 1-17.
630 <https://doi.org/10.4401/ag-6218>
- 631 Hamlin, R., Woodward, J., Black, S., Macklin, M.G., 2000. Sediment fingerprinting as a tool for interpreting long-
632 term river activity: the Voidomatis basin, NW Greece. In: Foster, I.D.L. (Ed.), Tracers in Geomorphology.
633 Wiley, Chichester, pp. 473-501. https://pure.manchester.ac.uk/ws/files/32295226/FULL_TEXT.PDF
- 634 Hauer, C., Skrame, K., Fuhrmann, M., 2021. Hydromorphological assessment of the Vjosa river at the catchment
635 scale linking glacial history and fluvial processes. Catena 207, 105598.
636 <https://doi.org/10.1016/j.catena.2021.105598>
- 637 Heinrich, H., 1988. Origin and consequences of cyclic ice rafting in the Northeast Atlantic Ocean during the past
638 130,000 years. Quat. Res. 29, 142-152. [https://doi.org/10.1016/0033-5894\(88\)90057-9](https://doi.org/10.1016/0033-5894(88)90057-9)
- 639 Hemming, S. R., 2004. Heinrich events: Massive Late Pleistocene detritus layers of the North Atlantic and their
640 global climate imprint. Rev. Geophys. 42, RG1005. <https://doi.org/10.1029/2003RG000128>
- 641 Hidy, A.J., Gosse, J.C., Pederson, J.L., Mattern, J.P., Finkel, R.C., 2010. A geologically constrained Monte Carlo
642 approach to modeling exposure ages from profiles of cosmogenic nuclides: an example from Lees Ferry,
643 Arizona. Geochem. Geophys. Geosyst. 11, 18.
644 <https://agupubs.onlinelibrary.wiley.com/doi/pdfdirect/10.1029/2010GC003084>
- 645 Hughes, P.D., 2010. Geomorphology and Quaternary stratigraphy: The roles of morpho-, litho-, and
646 allostratigraphy. Geomorphology, 123, 189-199.

- 647 Institutin Topografik te Ushtrise Tirana, 1990. Topographic maps of Socialist Republic of Albania in scale:
648 1:25000. Archive of Institute of Seismology, Tirana, Albania. (in Albanian).
- 649 Kallel, N., Paterne, M., Labeyrie, L.D., Duplessy, J.C., Arnold, M., 1997. Temperature and salinity records of the
650 Tyrrhenian sea during the last 18 000 years. *Palaeogeogr., Palaeoclimatol., Palaeogeogr., mat. Palaeoecol.*
651 135, 97–108. [https://doi.org/10.1016/S0031-0182\(97\)00021-7](https://doi.org/10.1016/S0031-0182(97)00021-7)
- 652 Kallel, N., Duplessy, J.C., Labeyrie, L., Fontugne, M., Paterne, M., Montacer, M., 2000. Mediterranean pluvial
653 periods and Sapropel formation over the last 200,000 years. *Palaeogeogr. Palaeoclimatol. Palaeoecol.*
654 157, 45-58. [https://doi.org/10.1016/S0031-0182\(99\)00149-2](https://doi.org/10.1016/S0031-0182(99)00149-2)
- 655 Koçi, R., 2007. Geomorphology of Quaternary deposits of Albanian rivers. Ph.D. Thesis. Archive of Institute of
656 Seismology, Tirana, Albania (in Albanian language) 217 p.
- 657 Koçi, R., Dushi, E., Begu, E., Bozo, R., 2018. Impact of tectonics on rivers terraces geomorphology in Albania.
658 Proceedings of the International Multidisciplinary Scientific GeoConference SGEM. pp. 189-196.
659 <https://doi.org/10.5593/sgem2018/1.1>
- 660 Konijnendijk, T.Y.M., Ziegler, M., Lourens, L.J., 2015. On the timing and forcing mechanisms of late Pleistocene
661 glacial terminations: insights from a new high-resolution benthic stable oxygen isotope record of the
662 eastern Mediterranean. *Quat. Sci. Rev.* 129, 308-320.
663 <https://doi.org/10.1016/j.quascirev.2015.10.005>
- 664 Korschinek, G., Bergmaier, A., Faesterman, T., Gerstmann, U.C., Knie, K., Rugel, G., Wallner, A., Dillmann, I.,
665 Dollinger, G., Lierse von Gostomski, C., Kossert, K., Maiti, M., Poutivsev, M., Remmert, A., 2010. A
666 new value for the half-life of ¹⁰Be by heavy-Ion elastic recoil detection and liquid scintillation counting.
667 *Nucl. Instrum. Methods Phys. Res. B* 268, 187-191. <https://doi.org/10.1016/j.nimb.2009.09.020>
- 668 Lal, D., 1991. Cosmic ray labeling of erosion surfaces: *In situ* nuclide production rates and erosion models. *Earth*
669 *Planet. Sci. Lett.* 104, 424-439. [https://doi.org/10.1016/0012-821X\(91\)90220-C](https://doi.org/10.1016/0012-821X(91)90220-C)
- 670 Lambeck, K., Chappell, J., 2001. Sea-level change through the last glacial cycle. *Sci.* 292, 679–686. DOI:
671 [10.1126/science.1059549](https://doi.org/10.1126/science.1059549)
- 672 Lewin, J., Macklin, M.G., Woodward, J.C., 1991. Late Quaternary fluvial sedimentation in the Voidomatis Basin,
673 Epirus, Northwest Greece. *Quat. Res.* 35, 103-115. [https://doi.org/10.1016/0033-5894\(91\)90098-P](https://doi.org/10.1016/0033-5894(91)90098-P)
- 674 Macklin, M.G., Lewin, J., Woodward, J.C., 1997. Quaternary river sedimentary sequences of the Voidomatis
675 Basin. In: Bailey, G.N. (Ed.), *Klithi: Palaeolithic Settlement and Quaternary Landscapes in Northwest*
676 *Greece. Klithi in its Local and Regional Setting*, vol. 2. McDonald Institute for Archaeological Research,
677 Cambridge, pp. 347–359.
678 https://pure.manchester.ac.uk/ws/portalfiles/portal/32298402/FULL_TEXT.PDF
- 680 Macklin, M.G., Fuller, I.C., Lewin, J., Maas, G.S., Passmore, D.G., Rose, J., Woodward, J.C., Black, S., Hamlin,
681 R.H.B., Rowa, J.S., 2002. Correlation of fluvial sequences in the Mediterranean Basin over last 200 ka
682 and their relationship to climate change. *Quat. Sci. Rev.* 21, 1633-1641.
683 [https://doi.org/10.1016/S0277-3791\(01\)00147-0](https://doi.org/10.1016/S0277-3791(01)00147-0)
- 684 Martin, L.C.P., Blard, P.-H., Balco, G., Lav' e, J., Delunel, R., Lifton, N., Laurent, V., 2017. The CREp program
685 and the ICE-D production rate calibration database: a fully parameterizable and updated online tool to
686 compute cosmic-ray exposure ages. *Quat. Geochronol.* 38, 25–49.
687 <https://doi.org/10.1016/j.quageo.2016.11.006>
- 688 Melo, V. 1961. Evidence of neotectonics movements in the Shkumbini terraces along the Elbasani-Peqini sector.
689 State University of Tirana. *Bull. Of Natural Sciences II*, 135-148.
- 690 Melo, V. 1996. The terraces of the Mat River. In: Aliaj, Sh., Melo, V., Hyseni, A., Skrami, J., Mëhillka, Ll. Muço,
691 B., Sulstarova, E., Prifti, K., Pashko, P., Prillo, S. Neo-tectonic map of Albania in scale 1:200000. Edited
692 by Archive of Seismology Institute, Tirana, Albania. (in Albanian).
- 693 Merchel, S., Herpers, U., 1999. An update on radiochemical separation techniques for the determination of long-
694 lived radionuclides via accelerator mass spectrometry. *Radiochim. Acta* 84, 215-219.
695 <https://doi.org/10.1524/ract.1999.84.4.215>
- 696 Meyer, G.A., Wells, S.G., Jull, A.J.T., 1995. Fire and alluvial chronology in Yellowstone National Park: Climate
697 and intrinsic controls on Holocene geomorphic processes. *Geol. Soc. America Bull.* 107, 1211-1230.
- 698 Noller, J.S., Sowers, J.M., Lettis, W.R., 2000. Quaternary geochronology: Methods and applications. American
699 Geophysical Union. Vol. 4, 582 pp. DOI:10.1029/RF004
- 700 North Greenland Ice Core Project Members, 2004. High-resolution record of Northern Hemisphere climate
701 extending into the last interglacial period, *Nature*, 431, 147–151, [doi:10.1038/nature02805](https://doi.org/10.1038/nature02805).
- 702 Obreht, I., Buggle, B., Catto, N., Marković, S.B., Bösel, S., Vandenberghe, D.A.G., Hambach, U., Svirčev, Z.,
703 Lehmkuhl, F., Basarin, B., Gavrilov, M.B., Jović, G., 2014. The Late Pleistocene Belotinac section
704 (southern Serbia) at the southern limit of the European loess belt: Environmental and climate

705 reconstruction using grain size and stable C and N isotopes. *Quaternary International*, 334-335, pp. 10-
706 19. <https://doi.org/10.1016/j.quaint.2013.05.037>

707 Olszak J, 2017. Climatically controlled terrace staircases in uplifting mountainous areas. *Glob. Planet. Change*
708 156, 13-23. <https://doi.org/10.1016/j.gloplacha.2017.07.013>

709 Ozenda, P. 1975. Sur les étages de végétation dans les montagnes du bassin méditerranéen. Documents de
710 cartographie écologique, XVI, 1-32. [http://ecologie-alpine.ujf-
711 grenoble.fr/articles/DCE_1975_16_1_0.pdf](http://ecologie-alpine.ujf-grenoble.fr/articles/DCE_1975_16_1_0.pdf)

712 Pashko, P., and Aliaj, S. (2020). Stratigraphy and Tectonic Evolution of Late Miocene - Quaternary Basins in
713 Eastern Albania: A Review. *geosociety* 56, 317–351. doi:10.12681/bgsq.22064.
714 [https://www.openarchives.gr/aggregator-openarchives/edm/geosociety/000068-
715 geosociety_article_view_22064](https://www.openarchives.gr/aggregator-openarchives/edm/geosociety/000068-geosociety_article_view_22064)

716 Pazzaglia, F.J., 2022. Fluvial Terraces. *Treatise on Geomorphology*, 6, pp. 639-673.
717 <https://doi.org/10.1016/B978-0-12-409548-9.12088-3>

718 Prifti K., 1981. Format Kuaternare të luginës së rrjedhës së sipërme të Vjosës dhe disa veçori karakteristike të tyre.
719 Përmbledhje studimesh Nr.2. (In Albanian language)

720 Prifti, K., 1984. Geomorphology of quaternary deposits of the Devoll River. *Buletini I Shkencave Gjeologjike* 2,
721 43-59. (in Albanian).

722 Prifti, K, Meçaj., N., 1987. Geomorphologic development of river valleys in Albania and their practice importance.
723 *Geographic Studies*2, 237-253

724 Rahmstorf, S., 2002. Ocean circulation and climate during the past 120 000 years. *Nature* 419, 207-214.
725 <https://www.nature.com/articles/nature01090>

726 Ramsey, B., 2009. Bayesian analysis of radiocarbon dates. *Radiocarbon* 51, 337-360. DOI:
727 [10.2458/azu_js_rc.51.3494](https://doi.org/10.2458/azu_js_rc.51.3494)

728 Rashid, H., Hesse, R., Piper, D.J., 2003. Evidence for an additional Heinrich event between H5 to H6 in the
729 Labrador Sea. *Paleoceanogr.* 18, 1077-1091. <https://doi.org/10.1029/2003PA000913>

730 Reimer, P.J., Bard, E., Bayliss, A., Beck, J.W., Blackwell, P.G., Bronk Ramsey, C., Grootes, P.M., Guilderson, T.
731 P., Hafliðason, H., Hajdas, I., HattĹ, C., Heaton, T.J., Hoffmann, D. L., Hogg, A.G., Hughen, K.A.,
732 Kaiser, K.F., Kromer, B., Manning, S.W., Niu, M., Reimer, R.W., Richards, D.A., Scott, E.M., Southon,
733 J.R., Staff, R.A., Turney, C. S.M., van der Plicht, J., 2013, IntCal13 and Marine13 Radiocarbon Age
734 Calibration Curves 0-50,000 Years cal BP. *Radiocarbon*, 55, 1869-1887.
735 https://doi.org/10.2458/azu_js_rc.55.16947

736 Repka, J.L., Anderson, R.S., Finkel, R.C., 1997. Cosmogenic dating of fluvial terraces, Fremont River, Utah. *Earth*
737 *Planet. Sci. Lett.* 152, 59-73. [https://doi.org/10.1016/S0012-821X\(97\)00149-0](https://doi.org/10.1016/S0012-821X(97)00149-0)

738 Riser J., under the direction of, 1999. *Le Quaternaire. Géologie et milieux naturels. Édité. Dunod, Paris, 320 p.*

739 Rixhon, G., 2022. A question of time: historical overview and modern thought on quaternary dating methods to
740 produce fluvial chronologies, *Quaternaire* 33, <https://doi.org/10.4000/quaternaire.16705>

741 Robertson, A., Shallo, M. 2000. Mesozoic-Tertiary tectonic evolution of Albania in its regional Eastern
742 Mediterranean context. *Tectonophys.* 316, 197-254. [https://doi.org/10.1016/S0040-1951\(99\)00262-0](https://doi.org/10.1016/S0040-1951(99)00262-0)

743 Roure, F., Nazaj, S., Mushka, K., Fili, I., Cadet, J.P., Bonneau, M., 2004. Kinematic evolution and petroleum
744 systems - An appraisal of the Outer Albanides. In: McClay K.R. (Ed.), *Thrust Tectonics and Hydrocarbon*
745 *Systems*, AAPG Memoir 82, pp. 474-493. <https://doi.org/10.1306/M82813C25>

746 Roucoux, K.H., Tzedakis, P.C., Frogley, M.R., Lawson, I.T., Preece, R.C., 2008: Vegetation history of the marine
747 isotope stage 7 interglacial complex at Ioannina, NW Greece. *Quat. Sci. Rev.* 27, 1378-1395.
748 <https://doi.org/10.1016/j.quascirev.2008.04.002>

749 Rowey, C., Siemens, M., 2021. Age constraints of the Middle Pleistocene till and loess sequence in
750 northeast Missouri, USA, based on pedostratigraphy within a polygenetic paleosol. *Catena* 203,
751 105294. <https://doi.org/10.1016/j.catena.2021.105294>

752 Sadori, L., Koutsodendris, A., Panagiotopoulos, K., Masi, A., Bertini, A., Combourieu-Nebout, N., Francke, A.,
753 Kouli, K., Joannin, S., Mercuri, A.-M., Peyron, O., Torri, P., Wagner, B., Zanchetta, G., Sinopoli, G.,
754 Donders, T.H., 2016. Pollen-based paleoenvironmental and paleoclimatic change at Lake Ohrid (south-
755 eastern Europe) during the past 500 ka. *Biogeosci.* 13, 1423-1437.
756 <https://bg.copernicus.org/articles/13/1423/2016/>

757 Sánchez Goñi, M.F., Cacho, I., Turon, J.-L., Guiot, J., Sierro, F.J., Peyrouquet, J.-P., Grimalt, J.O., Shackleton,
758 N.J., 2002. Synchronicity between marine and terrestrial responses to millennial scale climatic variability
759 during the last glacial period in the Mediterranean region. *Clim. Dyn.* 19, 95-105. DOI: [10.1007/s00382-
760 001-0212-x](https://doi.org/10.1007/s00382-001-0212-x)

761 Schaller, M., Ehlers, T., Stor, T., Torrent, J., Lobato, L., Christl, C., Vockenhuber, C., 2016. Timing of European
762 fluvial terrace formation and incision rates constrained by cosmogenic nuclide dating. *Earth and Planetary*
763 *Science Letters* 451, 221–231. <https://doi.org/10.1016/j.epsl.2016.07.022>

764 Schanz S. A, Montgomery D. R., Collins B.D., Duvall A.R., 2018. Multiple paths to straths: A review and
765 reassessment of terrace genesis. *Geomorphology*, 312, 12-23.
766 [https://www.researchgate.net/publication/324096035_Multiple_paths_to_straths_A_review_and_reasse](https://www.researchgate.net/publication/324096035_Multiple_paths_to_straths_A_review_and_reassessment_of_terrace_genesis)
767 [sment_of_terrace_genesis](https://www.researchgate.net/publication/324096035_Multiple_paths_to_straths_A_review_and_reassessment_of_terrace_genesis)

768 Schumm, S., 1979. Geomorphics thresholds: the concepts and its application. *Transactions of the Institute of*
769 *British Geographers*. 4, 485-515. <http://geomorphology.sese.asu.edu/Papers/Schumm%201979.pdf>

770 SRTM (2013). NASA Shuttle Radar Topography Mission Shuttle Radar Topography Mission (SRTM) Global.
771 Distributed by OpenTopography. <https://doi.org/10.5069/G9445JDF>

772 Starkel, L., 1994. Reflection of the Glacial-Interglacial Cycle in the evolution of the Vistula River Basin, Poland.
773 *Terra Nova* 6, 486-494. <https://doi.org/10.1111/j.1365-3121.1994.tb00892.x>

774 Stone, J.O., 2000. Air pressure and cosmogenic isotope production. *J. Geophys. Res.* 105(B10), 753-759.
775 <https://doi.org/10.1029/2000JB900181>

776 Toucanne, S., Minto'o, C., Fontanier, C., Bassetti, M-A, Jorry, S., Jouet, G., 2015. Tracking rainfall in the northern
777 Mediterranean borderlands during sapropel deposition. *Quaternary Science Reviews* 129, 178-195.
778 <https://doi.org/10.1016/j.quascirev.2015.10.016> <https://doi.org/10.1016/j.quascirev.2015.10.016>

779 Tzedakis, P.C., Frogley, M. R., Lawson, I. T., Preece, R. C., Cacho, I., de Abreu, L., 2004. Ecological thresholds
780 and patterns of millennial-scale climate variability: The response of vegetation in Greece during the last
781 glacial period. *Geology* 32, 109-12. <https://doi.org/10.1130/G20118.1>

782 Vandenberghe, 1993. River Terrace Development and its Relation to Climate: the Saalian Caberg Terrace of the
783 Maas River Near Maastricht (The Netherlands), *Mededelingen Rijks Geologische Dienst N.S.* 47., 19-24

784 Vandenberghe, J., 2003. Climate forcing of fluvial system development: an evolution of ideas. *Quaternary Science*
785 *Reviews* 22, 2053–2060. [https://doi.org/10.1016/S0277-3791\(03\)00213-0](https://doi.org/10.1016/S0277-3791(03)00213-0)

786 Vandenberghe, J., 2008. The fluvial cycle at cold-warm-cold transitions in lowland regions: a refinement of theory.
787 *Geomorphology* 98, 275-284. <https://doi.org/10.1016/j.geomorph.2006.12.030>

788 Vandenberghe, J., 2015. River terraces as a response to climatic forcing: Formation processes, sedimentary
789 characteristics and sites for human occupation. *Quaternary International* 370, 3-11.
790 <https://doi.org/10.1016/j.quaint.2014.05.046>

791 Vassallo R., J-F. Ritz, R. Braucher, M. Jolivet, A. Chauvet, C. Larroque, S. Carretier, D. Bourlès, C. Sue, M.
792 Todbileg, N. Arzhannikova and S. Arzhannikov, 2007. Transpressional tectonics and stream terraces of
793 the Gobi-Altay, Mongolia, *Tectonics*, vol. 26, TC5013, [doi:10.1029/2006TC002081](https://doi.org/10.1029/2006TC002081).

794 Wagner, B., Lotter, A.F., Nowaczyk, N., Reed, J.M., Schwalb, A., Sulpizio, R., Valsecchi, V., Wessels, M.,
795 Zanchetta, G., 2009. A 40,000-year record of environmental change from ancient Lake Ohrid (Albania
796 and Macedonia), *J. Paleolimnol.* 41, 407-430. [https://link.springer.com/article/10.1007/s10933-008-](https://link.springer.com/article/10.1007/s10933-008-9234-2)
797 [9234-2](https://link.springer.com/article/10.1007/s10933-008-9234-2)

798 Wagner, B., Vogel, H., Zanchetta, G., Sulpizio, R., 2010. Environmental change within the Balkan region during
799 the past ca. 50 ka recorded in the sediments from lakes Prespa and Ohrid. *Biogosci.* 7, 3187-3198.
800 <https://bg.copernicus.org/articles/7/3187/2010>

801 Wegmann, K.W., Pazzaglia, F.J., 2002. Holocene strath terraces, climate change, and active tectonics; the
802 Clearwater River basin, Olympic Peninsula, Washington State. *Geol. Soc. Am. Bull.* 114 (6), 731-744.
803 DOI: [10.1130/0016-7606\(2002\)114<0731:HSTCCA>2.0.CO;2](https://doi.org/10.1130/0016-7606(2002)114<0731:HSTCCA>2.0.CO;2)

804 Wegmann, K.W., Pazzaglia, F.J., 2009. Late Quaternary fluvial terraces of the Romagna and Marche Apennines,
805 Italy. *Quat. Sci. Rev.* 28, 137-165. <https://doi.org/10.1016/j.quascirev.2008.10.006>

806 Woodward, J.C., Hamlin, R.B.H., Macklin, M.G., Karkanis, P., Kotjabopoulou E., 2001. Quantitative sourcing of
807 slackwater deposits at Boila rockshelter: A record of late-glacial flooding and palaeolithic settlement in
808 the Pindus Mountains, Northern Greece. *Geoarchaeology* 16(5), 501-536.
809 <https://doi.org/10.1002/gea.1003>

810 Woodward, J.C., Hamlin, R.H.B., Macklin, M.G., Hughes, P.D., Lewin, J., 2008. Glacial activity and catchment
811 dynamics in northwest Greece: Long-term river behaviour and the slackwater sediment record for the last
812 glacial to interglacial transition. *Geomorphology* 101, 44-67. [10.1016/j.geomorph.2008.05.018](https://doi.org/10.1016/j.geomorph.2008.05.018)

813 Ziemen, F., Kapsch, M-L., Klockmann, M., Mikolajewicz, U., 2019. Heinrich events show two-stage climate
814 response in transient glacial simulations. *Clim. Past*, 15, 153–168. [https://doi.org/10.5194/cp-15-153-](https://doi.org/10.5194/cp-15-153-2019)
815 [2019](https://doi.org/10.5194/cp-15-153-2019)

816